DANMARKS OG GRØNLANDS GEOLOGISKE UNDERSØGELSE RAPPORT 2008/14

Ground check of airborne hyperspectral anomalies in the greater Mesters Vig area, central East Greenland

Bjørn Thomassen & Tapani Tukiainen

(1 DVD included)

GEOLOGICAL SURVEY OF DENMARK AND GREENLAND
MINISTRY OF CLIMATE AND ENERGY

G E U S

DANMARKS OG GRØNLANDS GEOLOGISKE UNDERSØGELSE RAPPORT 2008/14

Ground check of airborne hyperspectral anomalies in the greater Mesters Vig area, central East Greenland

Bjørn Thomassen & Tapani Tukiainen

(1 DVD included)

GEOLOGICAL SURVEY OF DENMARK AND GREENLAND
MINISTRY OF CLIMATE AND ENERGY

GEUS

Frontispiece. *Field spectroradiometer measurements in InterMoly's camp at Schuchert Gletscher. The Malmbjerg porphyry molybdenum deposit is in the background.*

Contents

Enclosed DVD

● Report text

● Map projection information and description of data formats
(Topographic background is GEUS' 1:100.000 standard maps)

● Map of hydrothermal alteration and mineralisation, Werner Bjerge
- Jarosite
- Ferric oxides (goethite)
- Clay minerals (illite, kaolinite)

● Map of hydrothermal alteration and mineralisation, Wegener Halvø
- Dolomitisation of Upper Permian carbonates

● Spectral library of the PIMA-field measurements

1. Abstract

In 2005, field work was carried out in the greater Mesters Vig area, central East Greenland, as a follow up to an airborne hyperspectral survey flown in 2000. The aim was to test the suitability of hyperspectral techniques to detect mineral occurrences and specific rock types in Arctic regions.

The field work was undertaken from fly camps in four areas underlain by Devonian–Palaeogene rocks. Twenty target localities were investigated comprising sedimentary base-metal deposits, subvolcanic porphyry molybdenum deposits and vein-type mineralisation. Collection of minerals and rocks for measurements with a field spectroradiometer was made in order to determine their spectral character and weathering products, and to compare these with the airborne data. Eighty-one reference samples were collected and analysed for 49 elements.

Mesters Vig area. This area is underlain by Carboniferous–Triassic sediments intruded by Palaeogene dolerite sills and dykes. Mineralisation comprises fault-controlled epithermal lead-zinc veins, including the mined-out Blyklippen deposit and stratabound zebra baryte. It was found that the SWIR-inactive mineralogy of the galena-sphalerite-bearing quartz veins and the carbonate-hosted baryte horizons makes their detection by airborne hyperspectral methods very difficult.

Werner Bjerge. The Palaeogene Werner Bjerge alkaline complex hosts widespread pneumatolytic–hydrothermal alteration, especially well developed at the Malmbjerg porphyry molybdenum deposit. The hyperspectral mapping confirmed the nature and extent of potassic high temperature hydrothermal alteration associated with the Malmbjerg granite stock. The mapping also defined a locality south of Werner Bjerge which displays many spectral similarities to Malmbjerg. This locality is an obvious follow-up target. Furthermore, the mapping revealed other distinct clusters of sulphide-bearing altered rocks which invite further investigation.

Kap Simpson area. The Palaeogene Kap Simpson alkaline complex hosts a major caldera structure displaying widespread alteration. Pyrite is common and traces of molybdenite are known. The hyperspectral survey confirmed the argillitic nature of the pyritised alteration zones. Furthermore, high temperature potassic alteration and greisen-like spectral signatures have been detected, offering new exploration targets.

Wegener Halvø. This peninsula comprises a mosaic of fault blocks exposing Neoproterozoic to Triassic sediments. Stratabound base-metal mineralisation occurs in Permo-Triassic sediments. A close association of dolomitisation with Upper Permian carbonate-hosted base-metal mineralisation has been confirmed by our investigations making the produced dolomite map useful for future exploration.

We conclude that there is good correlation between the airborne spectra and the field spectra, which confirms the spectral quality and stability of the hyperspectral airborne data.

In general, sulphide minerals have none or weak spectral response in the VNIR-SWIR spectral region whereas their potential alteration products, such as malachite, cerussite, smithsonite and jarosite, are distinctly SWIR-active. However, apart from jarosite, the alteration minerals of sulphides are virtually non-existent in the project area. On the other hand, the hyperspectral detection of wall-rock alteration related to mineralisation provides an effective method for outlining exploration targets, also in Arctic regions. This has been demonstrated by the present study.

2. Introduction

The present project *Ground check of airborne hyperspectral anomalies in the greater Mesters Vig area* aims at testing the suitability of hyperspectral techniques to detect mineral occurrences and specific rock types in Arctic regions. The project is a follow up on the *HyperGreen project* (see next section). It opened in the Spring 2005 with preparations for that summer's field work and is terminated by this report. The project has been financed by the Geological Survey of Denmark and Greenland (GEUS) and has benefitted through logistical co-operation with International Molybdenum Ltd. (InterMoly). This company conducted a major exploration campaign at the Malmbjerg molybdenum deposit south of Mesters Vig in 2005.

The field work covered four areas underlain by post-Caledonian rocks in central East Greenland: 1. Mesters Vig, 2. Werner Bjerge, 3. Kap Simpson and 4. Wegener Halvø (Map 1). These areas were originally selected for the *HyperGreen* airborne survey (section 3) because they host a number of known mineral occurrences. Areas 1–3 are in-side the National Park of North and North-East Greenland whereas area 4 is situated in Illoqqortoormiut/Scoresbysund municipality. The work was accomplished from July 6 to August 17 by the authors from four fly camps and from InterMoly's camps at Mestersvig airfield and Malmbjerg. Logistics and preliminary results have been reported by Thomassen (2005a). The weather and snow conditions were conducive to field work, and only four field days were lost due to bad weather.

3. Previous hyperspectral projects

Airborne hyperspectral measurements were carried out in central East Greenland in 2000 with HyVista Corp. as contractor (Tukiainen 2001). A Dornier 228 aeroplane from Deutsches Zentrum für Luft und Raumfart served as platform for the HyMap^{TM} hyperspectral spectrometer and a Zeiss aerial camera. The measurements had a resolution of 4 x 4 m nominal pixel size. The survey consisted of two projects:

- MINEO: *Assessing and monitoring the environmental impact of mining activities in Europe using advanced Earth observation techniques.* An EU-supported project directed towards mining-related pollution which included the abandoned lead-zinc mine Blyklippen at Mesters Vig. The project was completed in 2003 (Aastrup *et al.* 2001 a, b; Tamsdorf *et al.* 2003).

- HyperGreen: *Assessing the applicability of high resolution image spectroscopy as a mineral exploration tool.* A project to test the method's suitability in mineral exploration. This project, supported by the Bureau of Minerals and Petroleum (BMP), Government of Greenland, assessed airborne data from eight sub-areas with known mineral occurrences. The four southernmost of these have been investigated during the present project.

In 2001, follow-up field investigations on the two above projects were conducted in the Mesters Vig, Blyklippen and Kap Simpson areas.

4. Regional geology and mineralisation

Central East Greenland is dominated by the north–south trending Caledonian fold belt and coast-parallel rift basins with Late Palaeozoic and Mesozoic sediments and Palaeogene igneous rocks. The greater Mesters Vig area, as defined on Map 1, is underlain by Precambrian–Ordovician rocks, and post-Caledonian rocks of Devonian–Palaeogene age. The latter are Devonian to Lower Permian clastic sediments with minor intercalations of Devonian volcanics, Upper Permian to Cretaceous, mainly marine clastic and carbonate sediments, and Palaeogene intrusive and extrusive igneous rocks (Henriksen *et al.* 2000).

Mineral occurrences of the greater Mesters Vig area include 1) sedimentary deposits in carbonates and clastic sediments of Upper Permian and Triassic age, especially stratabound copper-lead-zinc together with baryte and quartz, 2) magmatic deposits associated with the Palaeogene intrusions in the Werner Bjerge and Kap Simpson areas, especially subvolcanic porphyry molybdenum deposits, and 3) vein-type mineralisation of uncertain age. A large number of quartz veins with variable concentrations of baryte, calcite, fluorite and lead-zinc-copper minerals occur in both magmatic and sedimentary rocks (Harpøth *et al.* 1986).

5. Follow-up work in 2005

The field work was planned in such a manner to ensure that as many different types of mineralisation as possible were investigated. There were three main targets. 1) Sedimentary deposits of stratabound copper-lead-zinc together with baryte and quartz in carbonates and clastic sediments of Upper Permian and Triassic age, 2) subvolcanic porphyry molybdenum deposits associated with the Palaeogene intrusions and 3) vein-type mineralisation of uncertain age with variable concentrations of lead-zinc-copper minerals and quartz, baryte, calcite and fluorite. As preparation for field work, a number of maps of significant primary minerals and alteration minerals were prepared on the basis of the airborne hyperspectral data: iron sulphides, iron oxides, malachite (Cu), smithsonite (Zn), cerrusite (Pb), clay minerals, quartz, baryte, calcite, dolomite and siderite. These maps, as well as all airborne raw data, were accessed in the field on CD-ROM.

For field measurements, a spectroradiometer borrowed from Geologische Bundesanstalt, Austria, was used: model PIMA II Infrared Spectroradiometer produced by Integrated Spectronics Pty. Ltd. (Frontispiece). The interpretation of the PIMA field spectra were done using PimaView 3.1 software by Integrated Spectronics Pty. Ltd. and ENVI's Spectral Analyst. The spectral libraries from USGS and Integrated Spectronics were used as reference for the mineral analysis and SAM (Spectral Angle Mapper/ENVI) processing of the hyperspectral data.

Each of the four field camps were located near known mineralisation and hyperspectral anomalies. These were localised and investigated during daily traverses, six days supported by helicopter lifts. Investigations comprised the collection of minerals and rocks for measurements with the field spectroradiometer in order to determine the spectral character of the rocks and their weathering products. At the same time, the airborne data were further processed in an iterative process of visualising of, and comparing with, the geological field observations. A selection of typical rocks and minerals were saved as reference samples.

Eighty-one reference samples were registered with GGU numbers 488401–53 and 488601–28. They are briefly described in Table 1 with GPS geographical co-ordinates; sample localities are indicated on Maps 2, 4, 6 and 7. The samples have been analysed for 49 elements by a combination of instrumental neutron activation (INNA) and inductively coupled plasma emission spectrometry (ICP) at Activation Laboratories Ltd., Ontario, Canada. Samples with high base-metal concentrations were subsequently assayed for the relevant elements. The analytical results are presented in Table 2.

6. Mesters Vig area

6.1 Geology and mineralisation

The Mesters Vig area is underlain by Carboniferous, Permian and Triassic sediments intruded by Palaeogene dolerite sills and dykes (Maps 2 and 3). Towards the south, the area is bordered by the Palaeogene Werner Bjerge alkaline complex; in the west, it is bordered by a major regional fault (Skeldal Fault) beyond which is the Caledonian fold belt.

Most of the area is made up of continental syn-rift deposits of Late Carboniferous to Early Permian age deposited in a N–S-orientated system of west-tilted half grabens belonging to the Mesters Vig Formation of the Traill Ø Group (Witzig 1954; Vigran *et al.* 1999). They form a 2–3 km thick unit of alluvial and fluvial sediments dominated by cross-bedded arkosic sandstones and conglomerates, with subordinate intercalations of lacustrine, calcareous and carbonaceous shales and mudstones with plant and fish fossils. The sequence dips about 20° to the north-east and is unconformably overlain by 250 m of the Upper Permian Foldvik Creek Group, mainly marine sediment. A basal conglomerate (Huledal Formation), marginal marine evaporites and carbonates (Karstryggen and Wegener Halvø Formations), bituminous shale (Ravnefjeld Formation) and a shallow marine clastic unit (Schuchert Dal Formation) compose this section that is overlain by Lower Triassic marine silty shales of the Wordie Creek Formation (Witzig 1954; Surlyk *et al.* 1986). The entire package is intruded by Palaeogene dolerite sills up to 100 m thick, two sets of dolerite dykes striking NNW and NNE, and lamprophyric dykes.

Faulting is widespread with the Mesters Vig Graben as the most conspicuous structure. This is 4 km wide and 12 km long and bordered by normal faults orientated NNW–SSE. Another dominant fault orientation is N–S. Upper Permian and Triassic sediments are down faulted *c.* 1000 m in the graben. It is evident that faulting has taken place at different times because displacement of the Upper Permian sediments is greater than that of the Palaeogene sills.

Fault-controlled epithermal lead-zinc veins are abundant over some 300 km^2 in the Mesters Vig area (Witzig 1954; Swiatecki 1981; Harpøth *et al.* 1986). Two major vein zones are associated with the border faults of the Mesters Vig Graben but other veins occur outside the graben.

The Sortebjerg–Blyklippen vein zone forms a discontinuous, 15 km long and 150°/80°E-orientated vein system along the western border fault of the graben. At its northern end, it hosts the Blyklippen deposit which was mined 1956–62. The Sortebjerg prospect at its southern end is the best investigated vein-section outside Blyklippen.

The Deltadal–Rungsted Elv vein zone is a discontinuous, 8 km-long vein system along the eastern border fault of the graben. It hosts 150°/80°W-orientated, strongly silicified and quartz-veined zones up to 50 m wide with lenses of massive galena up to 0.3 m thick.

Metal concentrations in mineralised vein intervals, as indicated by 10 m chip sample profiles, average about 4.2% Pb, 0.5% Zn and 0.3% Cu.

Vein mineralogy is dominated by quartz, baryte, galena and sphalerite, with minor calcite, pyrite and chalcopyrite, and traces of tetrahedrite. Sphalerite and galena occur as massive, coarse-grained lenses up to m-size but the minerals are rarely found together. Sphalerite and quartz often display rhythmic growth. The Pb/Ag ratio varies from 2,000 to 10,000 and there is a tendency for the ratio to decrease with increasing copper content. In some of the veins, there are indications of a vertical zonation involving upwards enrichments from quartz to baryte and from copper through zinc to lead, but no regional zonational pattern is evident. Wall-rock alteration of the Permo-Carboniferous sandstones comprises silicification and kaolinisation. Where the veins intersect Upper Permian sediments, extensive barytisation and silicification of the lowermost limestone unit may occur.

The paragenetic sequence for the Mesters Vig veins has three phases. The initial and main mineralising phase takes the form of quartz veining with major concentrations of sphalerite and galena, after which shearing and brecciation took place. The second phase embraces silicification and quartz cementing of the breccias and formation of baryte-bearing quartz veinlets, with minor amounts of sphalerite and galena, which intersect the main mineralisation. Finally, calcite veinlets were formed. The age of all mineralisation is assumed to be Palaeogene with the mineralising phases correlated with the intrusion of the Werner Bjerge alkaline complex. However, it should be noted that quartz veins have not been observed in rocks younger than Upper Permian and a Late Permian age for especially the early phase of mineralisation cannot be excluded.

6.2 Targets

Six pre-selected targets were investigated in the Mesters Vig area (Maps 2 and 3). The following brief descriptions are mainly based on Swiatecki (1981) and Harpøth *et al.* (1986).

Blyklippen Pb-Zn deposit

In 1948, galena-bearing quartz veins were discovered on the west coast of Mesters Vig by members of Danish expeditions to East Greenland (Lauge Koch Expeditions). This initial discovery led ultimately to mining at nearby Blyklippen, where a total of 545,000 tons of ore with 9.3% Pb and 9.9% Zn was produced between 1956 and 1962 (Bondam & Brown 1955; Fischer *et al.* 1958; Thomassen 2005b).

The Blyklippen lead-zinc deposit (‘The Lead Rock’), now exhausted, is part of the Sortebjerg–Blyklippen vein zone. The original deposit formed a sulphide lens at 300 m to 490 m a.s.l. within a major quartz-vein zone orientated 150°/40°–90°E developed along a normal fault in Permo-Carboniferous sandstones. The 1000 m-long zone is cut at the northern end by a transverse fault (040°/50° SE) and it gradually disappears to the south. Due to pinch-and-swell, its thickness varies from a few metres up to 50 m. The quartz-vein zone is sharply delineated to the east (along the hanging wall) by the fault. The western limit (the footwall) is less sharp, being a transitional zone with decreasing intensity of quartz veining and kaolinisation. Small-scale, late-stage, west-dipping faults intersect and brecciate the main quartz-vein zone. The main sulphide lens occurred close to the footwall of the zone within a swell structure at the northern end of the vein. There is no correlation between thickness of the quartz-vein zone and the sulphide lens.

The mined-out sulphide lens was 2–10 m thick, 300 m long and 160 m high. It consisted of 65% quartz, 15% sphalerite, 10% galena, 5–10% baryte with trace amounts of pyrite, chalcopyrite and tetrahedrite. Copper and silver contents were 120 ppm and 15 ppm, respectively. Across the lens, galena- and sphalerite-enriched sections alternated. In general, sphalerite was enriched in the lower and the northern part of the lens whereas galena was enriched near the surface and in the southern part. The 040° transverse fault delimiting the sulphide lens to the north hosts sheared and mylonitised ore lenses in the fault plane. The age of the faulting relative to the ore has been a matter of debate: either the transverse fault is pre-ore and thus the channel for the mineralising solutions, or it post-dates ore formation indicating the existence of a blind, transposed part of the ore body.

Activities and analytical results

The remnants of the mining town, tailings, adit portals and open pit were inspected in 2005 (Figure 1). No samples were collected, as this was done 2001 by one of the authors (GGU nos. 449301–04).

Sortebjerg

The Sortebjerg prospect is located at the southern end of the western border fault of the Mesters Vig Graben. Five outcrops occur over a distance of 4 km, each being a silicified, quartz-vein zone orientated 150°/80°E, 20–200 m long and up to 20 m wide. Galena and sphalerite occur as irregularly distributed pods and lenses which are generally concentrated along the hanging wall. The largest lens of massive galena is 13 m long and 0.75 m wide.

The prospect was trenched and drill-tested in 1952 (Håkansson 1953). Ground geophysics in 1954 gave only weak responses and a 1955 follow-up drill programme was left unfinished and unreported (Tegenholm 1954). Based on six diamond drill holes along one of the outcrops (Pings Elv), a resource of 220,000 tons with 9.3% Zn, 2.1% Pb and 0.7% Cu has been indicated over a length of 250 m.

Activities and analytical results

The vein-system was followed along strike for 2.7 km from Nedre Funddal to Deltadal. The four main outcrops are: Pings Elv Showing, Sorte Hjørne Showing, Flood River Showing and Mesters Vig River Showing.

The 1952 trenches and drill holes were localised. The holes are marked by casings. At Pings Elv, the dominant sulphide is brown sphalerite, often interbanded with vein quartz (Figures 2 and 3). At Sorte Hjørne, an up to 0.75 m thick lens of massive galena was noted (Figure 4). Three samples of sphalerite-bearing quartz vein from the Pings Elv Showing returned 2.8–41.6% Zn (488401; 488601, 02).

Holbergpasset

A part of the Deltadal-Rungsted Elv vein zone along the eastern border fault of the Mesters Vig Graben is exposed north of Holbergpasset, on the south slopes of Korsbjerg. The host rocks are Permo-Carboniferous sandstones and Upper Permian carbonates and clastic sediments.

Activities and analytical results

Quartz veins and Upper Permian sediments were investigated on the south slopes of Korsbjerg.

North of Holbergpasset, a quartz-baryte vein system up to 30 m thick with scattered galena and minor sphalerite and chalcopyrite is exposed along the eastern border fault of the Mesters Vig Graben (488408). Upper Permian carbonates occur on the hanging wall side of the vein c. 870 m a.s.l. but the contact is not exposed. The lower part of the sequence contains 3–5 m of white, porous, laminated limestone (488409). The upper part is homogeneous and partly silicified.

Additionally, smaller quartz veins occur west of the main vein in this area. Some 700 m to the south-west of the main vein outcrop, a quartz-baryte vein with minor sulphide is in direct contact with Upper Permian dolomitic limestone at c. 680 m a.s.l. The dolomitic limestone is homogeneous, laminated or brecciated and exhibits various stages of barytisation near the vein. The four samples collected contain 7.9–30.6% Ba (~13.4–52.0% baryte), 0.8–12.7% Ca and 0.2–6.1% Mg (488410–13). White, porous, laminated limestone is not exposed at this locality.

Lille Blydal

A mineralised quartz vein with NE-striking direction is located at the mouth of Lille Blydal.

Activities and analytical results

The quartz vein was found to be up to 3 m thick, with pinch-and-swell structure and nearly conformable with the bedding of the Permo-Carboniferous sandstone wall rock. It hosts massive pockets of coarse-grained sphalerite and galena. Two samples returned 0.04–7.3% Pb, 3.1–5.7% Zn and 0.2–0.4% Cu (488612–13).

Oksedal

In Oksedal south of Mesters Vig, the lower 5–9 m of the Upper Permian limestone sequence (Karstryggen Formation?) along a NNW-striking quartz vein (Oksedal Vein) is replaced by rhythmically banded, alternating mm–cm thick bands of grey and white baryte (zebra baryte) over a distance of up to 150 m from the vein. Based on mapping at 1:2000 and five shallow drill holes, a resource of some 350,000 tons with 90% baryte has been indicated in a near-surface part of this area (Thomassen 1980; Harpøth 1983).

Activities and analytical results

Zebra baryte hosted by the lower part of Upper Permian carbonates was investigated in 'Zebra Skar' and 'Bly Skar' (see map in Swiatecki 1981).

‘Zebra Skar’ exposes *c.* 2 m thickness of baryte-rich rocks, mainly developed as rhythmically banded zebra baryte (cf. the zebra textures of Wallace *et al.* 1994) (Figure 5). The zebra baryte consists typically of few mm thick, alternating white and grey bands, resembling bedding (Figure 7) but coarser banding, in places resembling cross bedding, also occurs. Microscopic and XRD investigations show that the white bands are baryte and the grey bands a mixture of baryte and fine-grained dolomite and calcite. Galena occurs sporadically, either as scattered blebs, or as 0.1–1.0 cm thick seams along baryte-dolomite contacts.

Five samples from ‘Zebra Skar’ returned up to 20.8% Pb, 14.0–36.0% Ba (~23.8–61.2% baryte), 1.6–9.9% Ca and 0.1–4.1% Mg (488438–42). High concentrations of baryte are difficult to assay by chemical methods, and the real baryte concentrations may well be higher. This is demonstrated by a gravimetric assay requested from Actlabs on 488441 which returned 41.0% Ba (~69.7% baryte) compared with the original INAA analysis of 31.2% Ba (~53.0% baryte).

Triaskæden

At the north-western end of Triaskæden, a north-south striking quartz vein (Albis Vein) intersects the Upper Permian sequence. The Upper Permian limestones have been silicified and partly replaced by baryte (zebra baryte) both on the slope towards Mesters Vig, and *c.* 1.5 km further to the south (‘Albis Kløft’), (Thomassen 1980, 1981).

Activities and analytical results

Zebra baryte hosted by Upper Permian carbonates were investigated in the south slope of ‘Albis Kløft’ (see map in Thomassen 1981). The main exposure at 500 m a.s.l. and a down faulted/slided ‘shoulder’ at 380 m a.s.l. were traversed.

At the main exposure west of the Albis Vein, baryte-bearing rocks can be followed laterally for a couple of hundred metres as sub-outcrops in a scree-covered slope. The baryte-bearing rocks are typical finely and coarsely rhythmically banded zebra baryte (488414, 17; Figure 8) and rocks with randomly orientated baryte crystals and minor disseminated galena (488415, 16). Four samples returned up to 0.26% Pb, 18.1–36.5% Ba (~30.8–62.1% baryte), 0.7–8.9% Ca and 0.1–0.3% Mg (488414–17). XRD-analysis of one sample (844814) at the Geological Institute, University of Copenhagen, gave 84% baryte, 9% calcite and 6% dolomite, indicating that Actlabs’ INAA barium results are too low (36.5% Ba ~62.1% baryte). A gravimetric assay from Actlabs showed 52.9% Ba (~89.9% baryte).

On the ‘shoulder’, a 2–3 m thick sequence of zebra baryte is exposed over *c.* 50 m laterally (Figure 6). Blocks of galena-bearing silicified limestone occur in the scree below this outcrop (488418–20). Similar galena-bearing, silicified rocks were found in sub-outcrop 4–5 m higher in the sequence of calcareous shale, on the rim of the plateau forming the ‘shoulder’ (844821). This rock is finely laminated with alternating, mm-thick laminae of galena and chert, and often brecciated (Figure 9). It is also characterised by significant concentrations of silver and antimony, in addition to lead. Four samples returned 8.5–41.1% Pb, 77–1570 ppm Ag, 76–2730 ppm Sb, 268–450 ppm As, 2.0–7.1% Ba (~3.4–12.1% baryte), 0.02–0.16% Ca and 0.02–0.05% Mg (488418–21).

6.3 Spectroradiometric measurements

Airborne hyperspectral data

The galena-sphalerite-bearing quartz veins make up a problematic target from an airborne hyperspectral mapping point of view since the characteristic mineralogy is predominantly SWIR (Short Wave Infra Red) inactive. This 'inactivity' may make the quartz veins detectable against the more SWIR-active wall rocks. However, the arkosic sandstones may contain especially quartz-rich layers making the interpretation more problematical. The presupposition for this type of mapping is that the veins have dimensions greater than 4 metres with good rock exposure. The sporadic Fe-oxide staining and kaolinitic alteration may contribute to the mapping/detection of these rocks. The rock types of the Blyklippen deposit, vegetation and tailing were extensively studied by the MINEO project (Aastrup *et al.* 2001b) outlining possible new targets similar to the known quartz veins.

Field spectroradiometric measurements

The mineralogy of the galena-sphalerite-bearing quartz veins is characterised by the predominance of SWIR-inactive minerals (quartz, baryte and sulphides). The field spectra in Figure 10 are typical examples on the spectral monotony of these rocks. The SWIR-active alteration products of sphalerite and galena (cerussite and smithsonite) have not been encountered. The marginal parts of the veins and wall rocks display a variable degree of kaolinisation which often is visible in the spectra. The content of calcite is very small and sporadic and does not have significant effect on the spectral properties.

The SWIR-spectras of baryte-rich rocks from Oksedal and Triaskæden demonstrate that these are variable and heterogeneous mixtures of baryte and/or calcite and dolomite (Figure 11). This means that the baryte-rich rock units probably are traceable on the basis of their content of SWIR active calcite and dolomite. However, the exposure geometry and restricted size of the known zebra baryte occurrences make their airborne hyperspectral detection questionable.

7. Werner Bjerge

7.1 Geology and mineralisation

The Werner Bjerge alkaline complex is part of the Palaeogene volcanic rifted margin that formed prior to, during, and after the onset of seafloor spreading in the North Atlantic. The complex forms a massif of alpine character which is roughly circular with a diameter of c. 17 km (Maps 1, 4 and 5). The complex is subvolcanic in character with a partially preserved roof of acid volcanics, chiefly feldspar porphyries, breccias and pyroclastic rocks. Among the intrusive rocks, three sub-complexes have been distinguished composed of basic rocks, alkali syenites and granites, and nepheline syenites (Bearth 1959). The basic sub-complex to the south-east, representing the roof zone of a gabbro intrusion, is the oldest and least known part of the Werner Bjerge complex. The nepheline syenite sub-complex to the south-west hosts a large nepheline-syenite body. The sub-complex of alkali syenites and granites to the north is probably the youngest part of Werner Bjerge. It hosts the molybdenum-bearing Malmbjerg and Mellempas granite stocks.

The complex is characterised by widespread pneumatolytic–hydrothermal alteration resulting in intense red and yellow colourations. Mineralisation is mainly associated with the northern sub-complex. Porphyry-type molybdenum mineralisation occurs at Malmbjerg and possibly also at Mellempas. Furthermore, scattered base-metal veins and skarns occur in the intrusive rocks and surrounding sediments. Niobium-REE mineralisation is known from boulder finds.

7.2 Targets

Five follow-up targets were examined in the Werner Bjerge. They form distinct sulphide anomalies in the airborne hyperspectral data. The following descriptions are mainly based on Bearth (1959), Geyti (1981) and Harpøth *et al.* (1986).

Malmbjerg

Malmbjerg is a 1750 m-high mountain located between two glaciers in the western part of Werner Bjerge. It hosts a porphyry-molybdenum deposit of the Climax-type, discovered in 1954 during systematic mapping by members of the Danish East Greenland Expeditions (Bearth 1959). Investigations in 1955–61 by Nordisk Mineselskab A/S, and in 1962 by a Nordisk Mineselskab/AMAX Inc. joint venture, involved the excavating of three adits totalling 1329 m, from where 146 holes were drilled, totalling some 22,000 m. An ore body of 119 Mt grading 0.25% MoS_2 at a cut-off of 0.17% MoS_2 was defined, but not found profitable at the molybdenum market price of the time. In 2004, Galahad Gold Plc acquired the property, spurred by a dramatic rise in the market price of molybdenum.

The Malmbjerg porphyry-molybdenum deposit is associated with a 25.7 Ma old, composite, alkali granite stock intruded into Carboniferous sandstones (Brooks *et al.* 2004). The stock is part of the intrusive Werner Bjerge alkaline complex and consists of three main lithological units: *perthite granite* with a quartz-feldspar porphyry roof phase (Arcturus porphyry), a heterogeneous *porphyritic aplite* (including the late Schuchert porphyry) and *porphyritic granites* in the lower part of the stock (Schassberger & Galey 1975). Molybdenite mineralisation occurs in a 700 x 700 x 150 m inverted bowel-shaped body located mainly in the perthite granite and its porphyritic roof phase. Molybdenite occurs in veinlets forming a stockwork of mutually offsetting veins. In addition, Mo-W-bearing greisen mineralisation occurs as flat-lying veins, up to one metre thick; minor base metals occur distally. Pronounced alteration is associated with the mineralisation, both inside, below and above the stockwork molybdenum mineralisation.

The Galahad subsidiary International Molybdenum Plc (InterMoly) conducted an impressive field programme in 2005 that included 4900 m of underground drilling (31 holes) and 1776 m channel sampling along the existing adits. The programme also involved geotechnical drilling, bulk-sampling, site studies for processing facilities, environmental studies and a full engineering study to determine the feasibility of moving the Malmbjerg deposit into commercial production. Based on the 2005 results and historical data, a mineral resource estimate was announced by InterMoly in November 2005. It indicates measured and indicated resources of 217 Mt at a grade of 0.20% MoS_2 using a 0.12% cut-off grade, including a higher-grade zone of 33.8 Mt at a grade of 0.28% MoS_2, above a cut-off of 0.25% (see InterMoly's home page).

Activities and analytical results

Parts of the slopes towards Schuchert and Arcturus glaciers were traversed (Figures 12 and 13). Typical stockwork and greisen mineralisation was studied in the Schuchert adit (Figures 14 and 15).

Three samples of mineralised drill core of perthite granite, Schuchert porphyry and greisen returned 987–1370 ppm Mo and 7–3630 ppm W (488449–51; Figure 16). A sample of stockwork mineralisation with coatings of yellow molybdic ochre (ferrimolybdit) returned 9670 ppm Mo and 54 ppm W (488619; Figure 17). A greisen sample returned 4580 ppm W and 19 ppm Mo (488618). Highly altered rocks (488616, 17, 20) and a clay zone in the Schuchert adit (488614) were also sampled.

Mellempas

In the Mellempas area, seven exposures of granite are interpreted to make up a single granite stock. This stock covering 15 km^2 intruded Carboniferous–Triassic sediments and syenites, porphyries and volcanic breccias of the alkali-syenite-granite sub-complex of the Werner Bjerge alkaline complex. The biotite granite forms a composite stock dominated by medium- to coarse-grained granite which has been intruded by quartz-feldspar porphyry and aplite. Prominent hydrothermal alteration in the area is reflected as colour anomalies caused by iron-oxide and manganese-oxide staining.

Mineralisation occurs as disseminated grains of molybdenite in the coarse-grained granite, and as vugs and pegmatites with molybdenite, wolframite, pyrite and fluorite in the coarse-grained granite and especially in the quartz-feldspar porphyry. Minor fine-grained molybdenite in veinlets exists in aplite. The mineralisation is believed to represent a roof-zone mineralisation (Geyti 1981).

Activities and analytical results
The ridge south-east of Mellempas (Røde Mur) and the largest nunatak north of Mellempas ('Mellemryg') were investigated (Figure 18).

At Røde Mur, aplite and quartz-feldspar porphyry were traversed. The granite in places contains 10–20% magnetite. Specks of molybdenite were observed in pegmatitic and aplitic phases of the granite. A sample of miarolitic aplite returned 208 ppm Mo (488403).

At 'Mellemryg', the south-eastern snout of the nunatak was traversed. The aplitic rock hosts stockwork-like quartz-pyrite mineralisation with minor fluorite and traces of galena and possibly molybdenite (488404–05).

Several molybdenite-bearing erratics found in Deltadal are supposed to originate from the Mellempas area. A sample from a 0.5 m block of brecciated aplite with coarse-grained molybdenite returned 2210 ppm Mo and 0.08% Sn (488402).

Jernhatten

Jernhatten in the northern sub-complex of the Werner Bjerge intrusion hosts alkali syenites covered by roof rocks of volcanic rhyolitic and syenitic breccias and porphyries, and exhibit distinct yellow and black colour anomalies caused by weathered pyrite and manganese oxides. A rhyolitic, fragmental boulder with pyrite-quartz veinlets and 633 ppm Mo was reported from this locality by Geyti (1981).

Activities and analytical results
The yellow colour anomaly on the north-western nose of Jernhatten was inspected (Figure 19). Fragmental rocks with disseminated pyrite are abundant at this locality. Two samples show no anomalous metal concentrations (488406, 07).

Jafet Gletscher

The Jafet Gletscher valley exposes Permo-Triassic sediments intruded by alkali syenites of the northern sub-complex of the Werner Bjerge intrusion. A few dm-wide epidotized fault zone with pockets of tremolite, baryte and galena in quartzitic sandstone has been reported from the west side of the glacier (Polesnig & Vohryzka 1958).

Activities and analytical results
The slopes on the west side of Jafet Gletscher were investigated (Figure 20). Red-brown weathered, baked Triassic shales rest on white, Upper Permian (?) sandstone. The baked shales are characterised by a well-developed weathering crust of goethite. Three scree

samples of pyrite-bearing, skarnoide and hornfelsed rocks are slightly anomalous in lead: 0.04–0.3% Pb (488422, 23; 488603).

Jass Gletscher

Jass Gletscher is surrounded by Triassic sediments, and syenites and volcanic breccias of the northern sub-complex of the Werner Bjerg intrusion. No mineralisation is known from this area.

Activities and analytical results

Part of the north-eastern slope and the terminal moraines of Jass Gletscher were searched for signs of mineralisation. Five samples of pyritiferous granites and syenites (488443–47) and one sample of quartz-calcite vein with minor galena-sphalerite (488448) were collected in the moraines. The chemical analyses show no significant metal concentrations in these samples.

7.3 Spectroradiometric measurements

Airborne hyperspectral data

The first assessment of the airborne hyperspectral data from the Werner Bjerge alkaline complex aimed to outline areas of hydrothermal alteration with a special interest in the potassic high-temperature alteration related to porphyry molybdenum deposits of the Climax-type. Other sulphide mineralised alteration zones and rock types are common in the Werner Bjerge alkaline complex. The predominating sulphide is pyrite. The preliminary assessment of the hyperspectral data therefore also included the mapping of iron sulphides (jarosite) and the alteration products of sphalerite (smithsonite) and galena (cerussite). Zones of pneumatolytic and hydrothermal alteration were mapped as the occurrence of biotite/phengite, illite, muscovite, kaolinite and goethite.

The hyperspectral mapping of the typical alteration products such as biotite, illite/muscovite, kaolinite, Fe-oxides, jarosite, chlorite etc. outlined a large number of targets with argillitic and propylitic alteration, with and without sulphides, as indicated by the presence of jarosite. The hyperspectral mapping did not detect targets with a spectral signature related to the occurrence of secondary minerals after galena and sphalerite (cerussite and smithsonite).

The preliminary hyperspectral mapping outlined the following major clusters of rocks with pneumatolytic and hydrothermal alteration, see also Map 5:

- Malmbjerg (‘Gelbe Rinne’)
- Mellempas
- Jaffet Gletcher
- Jernhatten area
- The basic sub-complex

- The outer contact zone of the Werner Bjerge complex, especially to the south
- A new locality south of Werner Bjerge

The detailed results of the mapping of pneumatolytic and hydrothermal alteration are shown as GIS-layers with the topographic map at 1:100 000 on the enclosed DVD.

Malmbjerg and Mellempas granite stocks

The Malmbjerg granite stock is recognised by a conspicuous high temperature potassic and siliceous hydrothermal alteration. Apart from affecting the stock itself, this also invades the roofing and surrounding Carboniferous sandstones to a distance of several hundreds of metres from the intrusion contact. This is well displayed by the MNF (Minimum Noise Fraction) transformed SWIR data of the HyMap survey, which illustrates a halo of the selected mineralogical characteristics (Figures 21 and 22). The high temperature alteration apparently culminated in the greisenisation of the granite stock, as exemplified by the topaz-enriched rocks in the roof of the granite stock (Figure 22). The HyMap data also indicate the presence of the greisen developments in the altered roofing sandstone. The hyperspectral data indicate that the Malmbjerg granite stock is either made up of two intrusive phases or it hosts an intensively hydrothermally affected roof phase.

The exposure of the Mellempas granite stock is restricted but Fe-oxide (with some jarosite) and kaolinite rich zones are clearly mapped by the HyMap data. There are vague scattered indications of greisenisation along the southern and northern margin of the stock (Map 5). The airborne hyperspectral data do not show any detectable hydrothermal alteration between the stock and the surrounding Carboniferous sandstones or the other rock units of the Werner Bjerge complex.

New exploration target

One locality *c.* 1 x 1.5 km in size located approximately 3.5 km to the south of Aldebaran Gletscher deserves special attention (Map 5, Figure 23). The Carboniferous sandstone in this area is affected by widespread hydrothermal alteration (illite, kaolinite, Fe-oxides, jarosite) including scattered spectral signature of greisen developments similar to those in the Malmbjerg granite stock. It is tempting to suggest that this locality could be the roof zone of a mineralised granite stock similar to the Malmbjerg stock.

Field spectroradiometric measurements

The field work confirmed the results from the airborne hyperspectral mapping which had outlined numerous targets with pneumatolytic–hydrothermal alteration with and without sulphides. The majority of the alteration zones are mixtures of clay minerals, hydrous iron oxides and iron sulphate. The zones of alteration could be classified in more detail if spectral unmixing was performed to determine the quantitative amounts of the alteration products. To what extent the mixtures are related to solely supergene processes is not known.

Field spectroradiometric measurements were done on material from the altered rocks of 'Gelbe Rinne' and the Malmbjerg granite stock (both GEUS and InterMoly samples). 'Gelbe Rinne' is the major, *c.* 600 m wide conspicuous alteration zone immediately to the north of the Malmbjerg granite stock. The zone displays an intense and varying degree of hydrothermal alteration; the most common alteration minerals are illite ($K_{0.6}(H_3O)_{0.4}Al_{1.3}Mg_{0.3}Fe^{2+}_{0.1}Si_{3.5}O_{10}(OH)_2{\bullet}(H_2O)$), quartz, goethite ($Fe^{3+}O(OH)$) and minor nontronite ($Na_{0.3}Fe^{3+}_2Si_3AlO_{10}(OH)_2{\bullet}4(H_2O)$) (Figures 24 and 25). The zone contains numerous enrichments of pyrite as indicated by jarosite ($KFe^{3+}_3(SO_4)_2(OH)_6$) (Figure 24). Iron oxide (goethite) staining gives the rocks a rusty colour and thereby enhances the visual impression of iron enrichment.

The rocks of the Malmbjerg granite stock are predominantly felsic (feldspar and quartz) with minor amounts of micas, amphiboles, iron oxides, pyrite, fluorite, molybdenite, and woframite. Weathered surfaces are invariably stained by Fe-oxides due to pyrite and/or the precipitation of Fe-oxide from surface waters. The spectra (examples in Figure 26) characterise the granite as a rather homogeneous muscovite/illite-bearing granite. In places the greisenisation (Figure 27) dramatically changes the SWIR spectral response from these rocks. This is due to the presence of topaz ($Al_2SiO_4(F,OH)_2$). In places the SWIR spectra display characteristics which indicate the presence of tourmaline ($NaFe^{3+}_3Al_6(BO_3)_3Si_6O_{18}(OH)_4$). The granite stock is dissected by a 60 cm-wide vertical clay zone exposed in the Schuchert adit (488614). The material is spectrally almost pure beidellite ($Na_{0.5}Al_{2.5}Si_{3.5}O_{10}(OH)_2{\bullet}(H_2O)$). Beidellite is a constituent of bentonitic clays, an alteration product in hydrothermal mineral deposits, especially porphyry Cu-Mo systems, and in soils derived from mafic rocks.

The characteristic SWIR field spectra from the Mellempas granite and aplite are shown in Figure 28. Apart from the overall reddish colour, which seems to be a more surfical phenomenon, the granite and aplite appear to be rather normal leucocratic rocks without particularly pronounced alteration. The characteristic feature of the Mellempas area is the presence of vertical, variably spaced NW–SE-striking shear zones. These zones are spectacularly coloured by blackish manganese oxide coatings and they host variable amounts of kaolinite and goethite. In places the alteration material is an almost pure whitish yellowish kaolinite (Figure 28). The field evidence seems to indicate that the quartz-feldspar porphyry is particularly subjected to kaolinitic alteration.

At Jernhatten, the field spectra (Figure 29) confirm the mineral detection from the airborne HyMap data: the bright yellow and yellowish orange-coloured alteration zones are made up of variable mixtures of jarosite, illite and quartz. Hydrous iron oxides (goethite) are ubiquitous as weathering products of pyrite.

At Jass Gletscher, the HyMap data indicate abundant jarosite/goethite-bearing rocks in the moraines of the glacier.

8. Kap Simpson area

8.1 Geology and mineralisation

The Palaeogene Kap Simpson intrusive complex is situated on the south-eastern headland of Traill Ø (Maps 1 and 6). It is intruded into Mesozoic clastic sediments and comprises a north-western alkali syenite part and a south-eastern zone consisting of sedimentary, volcanic and intrusive rocks surrounded by a syenitic ring-dyke system. The entire south-eastern part, the so-called ‘Dreibuchten Zone’, probably represents a caldera (Schaub 1942). The caldera-related igneous activity has three episodes: 1) an early volcanic episode, 2) an episode of syenite and granite intrusion and 3) a late volcanic episode.

Prominent alteration in the form of large colour-anomalous areas is widespread, particularly in the southern part of the caldera. Rocks within the colour-anomalous areas are typically pyritised, argillised and silicified and the occurrence of fluorite is a characteristic feature. It has been suggested that fumarolic activity was responsible for the major part of the alteration (Schaub 1942). Damtoft & Grahl-Madsen (1982) distinguish between a near-surface, fumarolic type of alteration and a deep-seated hydrothermal type. The colour anomalies were mapped during a Landsat-based remote sensing study but it was not possible to distinguish various types of alteration (Conradsen & Harpøth 1984). Traces of molybdenite are known from four localities where it occurs as scattered grains in quartz veinlets and disseminated in granite (Schassberger & Newall 1980; Damtoft & Grahl-Madsen 1982). Minor vein-type mineralisation with base metals and niobium occurs near intrusive contacts in the surrounding Mesozoic sediments.

8.2 Targets

Four follow-up targets were selected in the Kap Simpson complex. The following descriptions are mainly based on Schassberger & Newall (1980) and Damtoft & Grahl-Madsen (1982).

Upper Føndal

Upper Føndal is underlain by a mixture of caldera-related, hydrothermally-altered volcanic breccia and rhyolite, and intrusive rocks. A 300 m by 1500 m zone anomalous in molybdenum and pyrite has been outlined by detailed sampling and mapping on the north side of the valley. This zone could represent the outer and upper portion of a high-grade molybdenum deposit lying at depth under Føndal valley. The average molybdenum content of this zone is about 17 ppm Mo, about the same as the content of 22 ppm Mo of the outer portion of the Malmbjerg deposit (Schassberger & Newall 1980).

Activities and analytical results

The Upper Føndal molybdenum anomaly, indicated by 'Mo' on Map 6, was only observed from a distance (Figure 30). Characterised by a distinct red colour it was evident that snow cover in 2005 was smaller than in 1979 during the investigations by Schassberger & Newall (1980).

'Brogede Bjerg'

The distinct multi-coloured mountain at the northern end of Forårsdal – the 'Brogede Bjerg' of Damtoft & Grahl-Madsen (1982) – consists mainly of pyritised and hydrothermally altered, flow-banded volcanic breccias cut by various subvolcanic rocks. A sample of volcanic breccia with fluorite veinlets from the west side of the mountain has yielded 90 ppm Mo.

Activities and analytical results

Outcrops, as well as scree cones on the south slope of 'Brogede Bjerg' were searched for mineralisation and alteration types (Figure 31). Three pyritiferous samples (488425–27) returned nothing of interest, apart from 40 ppm Mo in a feldspar porphyry with pyrite veinlets (488425).

Forårsdal east

A cm-wide fluorite vein hosted by volcanic breccia with porphyritic sheets was sampled by Damtoft & Grahl-Madsen (1982). Molybdenite was not observed but three fluorite-rich grab samples returned 10–645 ppm Mo, 2–20 ppm W and 1.6–25.0% F.

Activities and analytical results

The ridge from which molybdenum-bearing fluorite had been reported by Damtoft & Grahl-Madsen (1982) was traversed. Fluorite was found outcropping at 294 m a.s.l. in an N–S-striking, few cm-thick vein or breccia zone in felsitic rocks. A composite sample returned 119 ppm Mo and 4 ppm W (488431). A scree block of vein fluorite in a fine-grained, brecciated volcanic rock found 30 m below returned 700 ppm Mo and <1 ppm W (488430). An altered, siliceous volcanic rock with traces of pyrite from an outcrop at the foot of the ridge returned 39 ppm Mo, 14 ppm W and 0.02% Sn (488607).

Forårsdal west

Part of the west side of Forårsdal is intensely stained red due to abundant pyrite, occurring in veinlets and disseminated in granitic and syenitic rocks. Trace amounts of molybdenite has been found disseminated and in quartz veinlets in these rocks (Damtoft & Grahl-Madsen 1982). Schassberger & Newall (1980) reported 90 ppm Mo in an aphanitic dyke rock from the same area.

Activities and analytical results

The lower part of the red-stained granite on the west side of Forårsdal was investigated (Figure 32). It consists of light grey, medium-grained, pyritiferous granite. Two samples of typical granite with 5–10% disseminated pyrite returned 10–11 ppm Mo (488424, 488610).

8.3 Spectroradiometric measurements

Airborne hyperspectral data

The two existing hyperspectral flight lines over the Kap Simpson complex cover the essential parts of the altered rocks of the 'Dreibuchten Zone' caldera (Map 6).

The preliminary hyperspectral mapping indicates that the intensive alteration is predominantly due to the presence of goethite and illite, along with scattered kaolinite-rich zones. The surface extent of the altered rocks is greatly enhanced by the intense weathering and dramatic topography. There is also some evidence of high temperature potassic alteration. On the basis of hyperspectral mapping of biotite, amphiboles and greisen-related minerals (topaz and muscovite), the following areas are outlined (see Map 6):

- Upper Føndal — High temperature potassic alteration
- North side of 'Brogede Bjerg' — High temperature potassic alteration
- Coast west of Forårsdal — High temperature potassic alteration
- East of Bredgletscher — Greisen-type alteration of granite

The zones of extensive hydrothermal alteration of the rocks of the 'Dreibuchten Zone' are readily mapped by the hyperspectral survey. The alteration is due to the formation of illite/nontronite, montmorillonite, quartz and highly variable amounts of hydrous Fe-oxides, manganese oxide and Fe-sulphate (jarosite), both as decomposition products of pyrite and of Fe-bearing rock-forming minerals. The kaolinitic alteration seems closely related to the pyritiferous medium-grained felsic sub-volcanic rocks occurring as dykes and minor irregular bodies in the rocks of the 'Dreibuchten Zone' and to the alkali syenite and granite in the central and north-western part of the Kap Simpson complex. These rocks are often altered to a mixture of kaolinite, jarosite and/or hydrous Fe-oxides.

The evidence of high temperature potassic alteration is vague. The known area of elevated Mo-content in Upper Føndal coincides with a weak indication from the hyperspectral mapping. The coastal area to the west of Forårsdal is intruded by a sheet-like body, which stands out with a spectral signature of high temperature potassic alteration. The marginal parts of the alkali syenite/granite show weak spectral evidence of greisen-like developments.

Field spectroradiometric measurements

The field spectroradiometric measurements confirm that the most characteristic alteration is related to the formation of illite and montmorillonite (Figure 33). The mutual amount of these minerals is apparently dictated by the composition of the host rock (montmorillonitic alteration products are typical for mafic material). The amount of iron, both as hydrous oxide (goethite) and sulfosalts (jarosite) is highly variable and intimately mixed with illite/montmorillonite.

The kaolinite-rich alteration zones are characteristically found in the pyritiferous medium-grained felsic sub-volcanic rocks occurring as dykes and minor irregular bodies (Figure 31).

9. Wegener Halvø

9.1 Geology and mineralisation

Wegener Halvø and Canning Land are two horst-like peninsulas in north-eastern Jameson Land comprising a complex pattern of fault blocks (Maps 1 and 7). Due to different elevations of these blocks a surprisingly comprehensive stratigraphical record is exposed within this relatively small area. Sediments of Neoproterozoic, Cambrian, Devonian, Carboniferous, Permian and Triassic ages, as well as Devonian granite and volcanics, and Tertiary dolerite dykes, are exposed (Noe-Nygaard 1934, 1937; Alexander-Marrack & Friend 1976; Clemmensen 1980; Surlyk *et al.* 1986; Stemmerik 1991).

The two peninsulas host a wide range of mineral deposit types: stratiform copper in Neoproterozoic and Triassic shales, stratiform base metals in Upper Permian shales, stratabound base metals in Upper Permian carbonates and Triassic sandstones, uranium in Devonian sandstones, disseminated gold-arsenic-bismuth-tungsten-base metals in Devonian granite and gold-base-metal-bearing veins in Neoproterozoic–Devonian rocks (Thomassen *et al.* 1982; Harpøth *et al.* 1986).

The Devondal area of southern Wegener Halvø (Map 7) is underlain by Devonian–Triassic sediments. The mainly marine Upper Permian Foldvik Creek Group is up to 300 m thick and rests with a distinct angular unconformity on continental Mid–Upper Devonian clastic sediments (Figure 34). The Foldvik Creek Group is dominated by an up to 250 m thick carbonate sequence (Karstryggen and Wegener Halvø Formations) with local black shale basins (Ravnefjeld Formation). The carbonates of The Wegener Halvø Formation comprise bryozoan build-ups (bioherms) and bedded flank deposits. Base metal mineralisation occurs in the black shales of Ravnefjeld Formation and in the carbonates of the Wegener Halvø Formation.

The Triassic Scoresby Land Group rests conformably on the uppermost clastic unit of the Foldvik Creek Group (Figure 35). It is more than 1000 m thick, composed of shallow marine to continental and lacustrine clastic sediments with intercalations of evaporites and thin carbonate beds. Base-metal mineralisation of stratiform or stratabound character occurs at four stratigraphical levels in the Devondal area.

9.2 Targets

Five targets had been selected in the Devondal area. The following brief descriptions are mainly based on Thomassen *et al.* (1982) and Harpøth *et al.* (1986).

Wegener Halvø Formation (Upper Permian)

Copper-lead-zinc-silver mineralisation is associated with quartz and baryte in the uppermost part of the carbonate build-ups and surrounding flank sediments. The sulphides are tennantite, chalcopyrite, galena, sphalerite and pyrite. Widespread silicification, dolomitisation and barytisation are associated with the mineralisation, and the intensity of the mineralisation increases to the east in Devondal. The largest single vein, which occurs in 'Knøvsen' in the east, is up to 5 m wide and outcrops for 400 m along strike. It is characterised by drusy quartz and a lateral zonation with baryte-copper to the west and a dominance of quartz-copper-lead-zinc to the east. 'Knøvsen' is also characterised by intense dolomitisation of limestone (H.K. Schönwandt, pers. comm. 1979). Twenty chip samples from 'Knøvsen' from a 100 x 500 m area average 0.5% Cu, 0.2% Pb and 0.1% Zn.

Activities and analytical results

This unit was investigated in southern, eastern and western Devondal (Figures 36 and 37).

Seven well-mineralised rock samples returned the following maximal values: 7.8% Cu, 2.4% Pb, 13.2% Zn, 110 ppm Ag, 7.2% Fe, 8.7% S, 0.88% As, 0.03% Sb, 14.4% Ba and 0.58% Sr (488432–37; 488622)

Klitdal Member (Lower Triassic)

Copper-silver and lead mineralisation of red-bed type occurs in alluvial fan deposits of pink and red, cross-bedded conglomerates and pebbly arkoses with subordinate mudstones and caliche horizons. The c. 250 thick sequence in southern Devondal hosts disseminated sulphides in 0.5–3 m thick beds at two levels. The main ore minerals are argentiferous chalcocite-covellite and galena. Copper- and lead-mineralised beds occur separately, except in remobilised veinlets, and both vertical and lateral zonation is evident. Copper-mineralised beds are estimated to contain 0.1–1.0% Cu and 5–80 ppm Ag, lead mineralised beds 2.0–2.5% Pb.

Activities and analytical results

This member was traversed in southern Devondal (Figures 38 and 39).

The following maximal values were returned from three arkose samples with abundant disseminated chalcocite and galena: 7.6% Cu, 14.3% Pb, 0.02% Zn, 327 ppm Ag, 0.53% Fe and 5.3% S (488453; 488621, 28).

Gråklint Beds (Middle Triassic)

Minor disseminated base-metal mineralisation occurs scattered in black shales, calcareous sandstones and limestones of the 5–30 m thick, cliff-forming Gråklint Beds. This unit represents a brief marine episode in the continental–lacustrine Middle Triassic sequence. Galena and pale sphalerite are the main sulphides, chalcopyrite and pyrite occur in variable amounts. Metal concentrations are modest and rarely exceed 1–2% combined lead-zinc-copper.

Activities and analytical results
This unit was investigated in southern Devondal.

A metre-thick unit of red and blue jasper was noted in the arkoses a few metres below the calcareous, cliff-forming sediments of the Gråklint Beds. Samples comprise a non-mineralised, laminated limestone from Gråklint Beds (488624) and a gypsum nodule from the overlaying gypsiferous sandstones and shales of the Gipsdalen Formation (488625; Figure 40).

Pingel Dal Beds (Upper Triassic)
The Pingel Dal Beds form a 20–40 m thick unit of red sandstone and siltstone, green mudstone, yellow dolostone and stromatolitic limestone indicating a shallow lacustrine depositional environment. The strata are overlain by the Malmros Klint Member (see below). Stratiform, fine-grained disseminations of chalcocite occur in the uppermost *c.* 1.5 m thick, light-coloured (reduced) bed of the Pingel Dal Beds. The mineralisation shows an extreme lateral persistency with typical contents of 0.1–0.2% Cu.

Activities and analytical results
This unit was investigated in southern Devondal.

A non-mineralised sample of oolitic dolomite mudstone was collected (488623).

Malmros Klint Member (Upper Triassic)
This member is composed of 200 m red mudstones of playa flat origin that grade upwards into more sandy, distal floodplain deposits. Copper mineralisation is located in the transition zone. Pale beds 0.1–1.0 m thick of cross-laminated sandstone intercalated with red mudstone host plant fragments, as well as plates and blebs of native copper and copper arsenides up to 10 cm long. The mineralised beds average *c.* 500 ppm Cu.

Activities and analytical results
The lowermost *c.* 100 m of this unit was investigated in southern Devondal.

A non-mineralised red mudstone was sampled (488626).

9.3 Spectroradiometric measurements

Airborne hyperspectral data
The airborne hyperspectral survey was hampered by extensive snow cover. However it covers most of Wegener Halvø but the coverage in the Devondal area is incomplete.

The survey covers the main outcrops of the Wegener Halvø Formation. Dolomite is the most SWIR-active mineral related to the carbonate-hosted copper-lead-zinc-silver mineralisation in this formation. The dolomite was mapped using the Spectral Angle (SAM) method.

The limestones mapped as the most intensively dolomitised correlate well with the known major occurrences of copper-lead-zinc mineralisation in the Devondal area (Figure 41). Dolomitisation is detected within the formation all over Wegener Halvø but it seems to be rather patchy and discontinuous (Figure 42). The detailed results of the mapping of dolomite are shown as GIS-layers with the topographic map at 1:100 000 on the enclosed DVD.

In red-bed type copper-silver-lead mineralisation of the Klitdal Formation, the most SWIR active minerals are malachite and calcite. The malachite staining is very patchy and hardly sufficiently developed to be detected by the airborne hyperspectral survey. The mineralised arkose contains some calcite but whether or not the presence of calcite is a diagnostic feature for this mineralisation is not known. Also it is uncertain whether the amount of carbonate is sufficient to be detected by the airborne hyperspectral survey. Furthermore, the mineralised locality in southern Devondal had particularly heavy snow cover at the time of hyperspectral data acquisition.

The base-metal mineralisation in the Gråklint Beds, Pingel Dal Beds and Malmros Klint Member could not be distinguished in the airborne data.

Field spectroradiometric measurements

The field spectroradiometric measurements on carbonates from the Wegener Halvø Formation show that calcitic limestone displays a variable degree of dolomitisation in the upper part of the formation. The dolomitisation at local scale may be very patchy and discontinuous. The mineralised units seem to be associated with the more intense dolomitisation which is clearly seen at ‘Knøvsen’ where the field measurements show that the calcite/dolomite ratio may be up to 40/30 (Figure 43).

The field SWIR spectra from mineralised and unmineralised arkose from the Klitdal Member are shown in Figure 44. The rocks typically contain calcite (up to 15%), but it is not known whether or not the presence of calcite is indicative for the mineralisation.

The SWIR spectrum of laminated limestone from the Gråklint Beds shows that it is made up of calcite with a variable amount of siliciclastic material. The SWIR spectrum from a gypsum nodule from Gipsdalen Formation is virtually a pure mineral spectrum showing that the nodules are made up pure gypsum (Figure 43). The SWIR spectrum from Pingel Dal Beds confirms the dolomitic character of this mudstone.

10. Conclusions and recommendations

The sound correlation between the airborne HyMap spectra and the field spectra from selected localities confirms the spectral quality and stability of the hyperspectral data generated by the HyMap-scanner.

The mineralogy of the primary target commodities of the present survey: sphalerite, galena, chalcopyrite, chalcocite, molybdenite and baryte are unfavourable for hyperspectral mapping with a spectral range of 350–2500 nm. These minerals have none or weak spectral response in the VNIR-SWIR spectral region. The potential alteration products of the sulphides, such as malachite, cerussite, smithsonite and jarosite are distinctly SWIR-active. Apart from jarosite, the alteration minerals of sulphides are virtually non-existing in the project area. Malachite staining is sporadically met with but the weak intensity and modest surface expression of malachite staining provides an insufficient spectral response for the present hyperspectral survey.

The quantitative detection of wall-rock alteration related to mineralisation provides an effective method for outlining of exploration targets. This has been demonstrated in the Wegener Halvø area where the hyperspectral based mapping of dolomitisation in the Upper Permian Wegener Halvø Formation has pinpointed localities with base-metal mineralisation.

The immediate conclusions and recommendations for future work in the four study areas are given below.

10.1 Mesters Vig area

The SWIR-inactive mineralogy of the galena-sphalerite-bearing quartz veins makes their detection by airborne hyperspectral methods problematic and ambiguous. When well exposed and of reasonable size, the lack of SWIR absorption features is less decisive and they may still be detectable as a contrast against the more SWIR-active wall rocks, soil and vegetation. The wall rock is in most instances sandstone which may contain nearly pure quartz lithologies. These are mineralogically similar to the barren quartz veins and can confuse the picture. The reported kaolinisation adjacent to the quartz veins could be used as mapping tool but the extent and persistency of the kaolinisation is not known.

The field spectra from zebra baryte indicate that the rock invariably contains considerable amounts of calcite and/or dolomite. The carbonate content, particularly the dolomite-rich varieties, may be used to trace potential baryte horizons. However, the illumination geometry and the exposure size of the known occurrences make their detection very difficult.

10.2 Werner Bjerge

The hyperspectral mapping has confirmed the nature and extent of the potassic high temperature hydrothermal alteration associated with the Malmbjerg granite stock. The mapping also outlined a locality in the Carboniferous sandstone *c.* 3.5 km to the south of the Werner Bjerge complex which in terms of SWIR-spectral characteristics displays many similarities to the Malmbjerg stock. This locality constitutes an obvious follow-up target.

Zones of hydrothermal alteration are common throughout the Werner Bjerge complex and the hyperspectral mapping has outlined distinct clusters of sulphide-bearing altered rocks in the various intrusive units. In particular, the unvisited alteration zones in the south-eastern part of the complex invite to further investigations.

10.3 Kap Simpson area

The airborne hyperspectral data cover the essential part of the hydrothermally altered rocks of the 'Dreibuchten Zone' caldera. The argillitic nature of the pyritised alteration zones has been confirmed and the variations in the alteration mineralogy seem to reflect the mineralogy of original rocks that range from rhyolite to andesite/dacite.

There are some weak indications of a high temperature potassic hydrothermal activity in the caldera, and greisen-like spectral signatures have been detected in the north-western marginal parts of the alkali syenite/granite of the Kap Simpson complex. They constitute new exploration targets.

10.4 Wegener Halvø

The close association of dolomitisation with the Upper Permian base-metal mineralisation has been confirmed by the investigations of the present project. The mapped dolomitised carbonates of the Wegener Halvø Formation remain targets for further exploration.

11. Acknowledgments

The staffs of International Molybdenum Ltd. (InterMoly), Polar Logistics Group (Polog) and Air Greenland A/S are thanked for efficient logistic cooperation and for enjoyable company in the Malmbjerg and Mestersvig camps. Klemens Grösel, Geologische Bundesanstalt, Austria, is thanked for the loan of the field spectrometer. Peter R. Dawes is thanked for his prompt response by going through this report, improving the English and making other suggestions for improvement. Only the authors are responsible for any defects that may remain.

12. References

Aastrup, P., Tamsdorf, M. & Tukiainen, T. 2001a: Blyklippen lead-zinc mine, Mestersvig. Existing knowledge. Mineo site Report. Danmarks og Grønlands Geologiske Undersøgelse Rapport **2001/115**, 39 pp.

Aastrup, P., Tamsdorf, M. & Tukiainen, T. 2001b: MINEO. Use of hyperspectral data for monitoring pollution from the lead-zinc mine, Mestersvig, in Northeast Greenland. In: Olsen, H.K., Lorentzen, L. & Rendal, O. (eds): Mining in the Arctic, 25–28. Lisse, The Netherlands: A.A. Balkema Publishers.

Alexander-Marrack, P.D. & Friend, P.F. 1976: Devonian sediments of East Greenland III. Meddelelser om Grønland **206**(3), 122 pp.

Bearth, P. 1959: On the alkali massif of the Werner Bjerge in East Greenland. Meddelelser om Grønland **153**(4), 62 pp.

Bondam, J. & Brown, H. 1955: The geology and mineralisation of the Mesters Vig area, East Greenland. Meddelelser om Grønland **135**(7), 40 pp.

Brooks, C.K., Tegner, C., Stein, H. & Thomassen, B. 2004: Re-Os and 40Ar/39Ar ages of porphyry molybdenum deposits in the East Greenland volcanic-rifted margin. Economic Geology **99**, 1215–1222.

Clemmensen L.B. 1980: Triassic rift sedimentation and paleogeography of central East Greenland. Bulletin Grønlands Geologiske Undersøgelse **136**, 72 pp.

Conradsen, K. & Harpøth, O. 1984: Use of Landsat multispectral scanner data for detection and reconnaissance mapping of iron oxide staining in mineral exploration, central East Greenland. Economic Geology **79**, 1229–1244.

Damtoft, J.S. & Grahl-Madsen, L. 1982: Geological and VLF-geophysical mapping of the Bredehorn Ba-Pb Prospect and preliminary mapping on SE Traill Ø for porphyry molybdenum mineralisation. Internal report, Nordisk Mineselskab A/S, 75 pp. (in archives of Geological Survey of Denmark and Greenland, GEUS Report File 20722).

Fischer, B., Heide, E. & Kirchner, G. 1958: Der Blei-Zink-Bergbau Mesters Vig in Ostgrönland. Berg- und Hüttenmännische Monatshefte **103**(8), 145–153.

Håkansson, S. 1953: Rapport over blottningsarbetena vid Sorte Bjerg – Mesters Vig – Grönland. Internal rapport, Nordisk Mineselskab A/S, 31 pp. (in archives of Geological Sur-vey of Denmark and Greenland, GEUS Report File 20611).

Harpøth, O. 1983: Summary of detailed chip sampling of the Bredehorn and Oksedal baryte occurrences, NM-Note 1/83. Internal report, Nordisk Mineselskab A/S, 31 pp. (in archives of Geological Survey of Denmark and Greenland, GEUS Report File 20788).

Harpøth, O., Pedersen, J.L., Schønwandt, H.K. & Thomassen, B. 1986: The mineral occurrences of central East Greenland. Meddelelser om Grønland, Geoscience **17**, 139 pp.

Henriksen, N., Higgins, A.K., Kalsbeek, F. & Pulvertaft, T.C.R. 2000: Greenland from Archaean to Quaternary. Descriptive text to the Geological map of Greenland, 1:2 500 000. Geology of Greenland Survey Bulletin **185**, 93 pp.

International Molybdenum's Home page: www.intermoly.com

Nielsen T.F.D 1987: Tertiary alkaline magmatism in East Greenland: a review. In: Fitton, J.G. & Upton, B.G.J. (eds): Alkaline igneous rocks. Geological Society Special Publication (London) **30**, 489–515.

Nielsen, T.F.D. 2002: Palaeogene intrusions and magmatic complexes in East Greenland, 66 to 75°N. Danmarks og Grønlands Geologiske Undersøgelse Rapport **2002/113**, 249 pp.

Noe-Nygaard, A. 1934: Stratigraphical outlines of the area round Fleming Inlet (East Greenland). Meddelelser om Grønland **103**(1), 88 pp.

Noe-Nygaard, A. 1937: Die palaeozoischen Eruptivgesteine von Canning Land. Meddelelser om Grønland **118**(6), 153 pp.

Polesnig, W. & Vohryzka, K. 1958: Die Erzvorkommen der Nördlichen Wernerberge, Aufnahmsbericht 1958. Internal report, Nordisk Mineselskab A/S, 19 pp. (in archives of Geological Survey of Denmark and Greenland, GEUS Report File 20751).

Schassberger, H.T. & Galey, J.T. 1975: Report on the 1974 core relogging Erzberg project, East Greenland. Internal report, AMAX Exploration, Inc., 40 pp. (in archives of Geological Survey of Denmark and Greenland, GEUS Report File 20667).

Schassberger, H.T. & Newall, G.C. 1980: The East Greenland molybdenum project, 1979. Internal report, AMAX Exploration of U.K. Inc., 53 pp. (in archives of Geological Survey of Denmark and Greenland, GEUS Report File 20151).

Schaub, H.P. 1942: Zur Geologie der Traill Insel (Nordost-Grönland). Eclogae Geologiae Helvetiae **35**, 1–54.

Stemmerik, L. 1991: Reservoir evaluation of Upper Permian build-ups in the Jameson Land basin, East Greenland. Rapport Grønlands Geologiske Undersøgelse **149**, 23 pp.

Surlyk, F., Hurst, J.M., Piasecki, S., Rolle, F., Scholle, P.A., Stemmerik, L. & Thomsen, E. 1986: The Permian of the western margin of the Greenland Sea – A future exploration tar-get. In: Halbouty, M.T. (ed.) Future petroleum provinces of the world. American Association of Petroleum Geologists Memoir **40**, 629–659.

Swiatecki, A. 1981: Prospecting of the Pb-Zn-Cu mineralised veins, Mesters Vig area, and drill programme Oksedal baryte body, Mesters Vig south, East Greenland, 1980, 10/80. Internal report, Nordisk Mineselskab A/S, 121 pp. (in archives of Geological Survey of Denmark and Greenland, GEUS Report File 20645).

Tamsdorf, M., Tukiainen, T. & Aastrup, P. 2003: MINEO arctic environment test site. Contamination/impact mapping and modelling. Final report. www.brgm.fr/mineo, 87 pp.

Tegenholm, R. 1954: Utlåtende over geo-elektriske mätninger vid Mesters Vig, Östgrönland. Internal report, Nordisk Mineselskab A/S, 6 pp. (in archives of Geological Survey of Denmark and Greenland, GEUS Report File 20629).

Thomassen, B. 1980: Prospecting of the Permian sediments of the Wegener Halvø, Mesters Vig south and Schuchert Dal areas, East Greenland, NM 1/1979. Internal report, Nordisk Mineselskab A/S, 70 pp. (in archives of Geological Survey of Denmark and Greenland, GEUS Report File 20704).

Thomassen, B. 1982: Prospecting for Cu-Pb-Zn-Ag-Au in the Upper Permian sediments and Devonian volcanics of East Greenland, NM 1–2. Internal report, Nordisk Mineselskab A/S, 100 pp. (in archives of Geological Survey of Denmark and Greenland, GEUS Report File 20702).

Thomassen, B. 2005a: The Blyklippen lead-zinc mine at Mesters Vig, East Greenland. Geology & Ore **5**, 12 pp. Copenhagen: Geological Survey of Denmark and Greenland.

Thomassen, B. 2005b: Feltrapport for Mestersvig 2005 projektet. Internal report, Danmarks og Grønlands Geologiske Undersøgelse, 6 pp.

Thomassen, B., Clemmensen, L.B. & Schønwandt, H.K. 1982: Stratabound copper-lead-zinc mineralisation in the Permo-Triassic of central East Greenland. Bulletin Grønlands Geologiske Undersøgelse **143**, 42 pp.

Tukiainen, T. 2001: Projects MINEO and HyperGreen: airborne hyperspectral data acquisition in East Greenland for environmental monitoring and mineral exploration. Geology of Greenland Survey Bulletin **189**,122–126.

Vigran, J.O., Stemmerik, L. & Piasecki, S. 1999: Stratigraphy and depositional evolution, Devonian–Carboniferous of Greenland. Palynology **23**, 115–152.

Wallace, M.W., Both, R.A., Ruano, S.M., Hach-Ali, P.F. & Lees, T. 1994: Zebra textures from carbonate-hosted sulphide deposits: sheet cavity networks produced by fracture and solution enlargement. Economic Geology **89**, 1183–1191.

Witzig, E. 1954: Stratigraphische und tektonische Beobachtungen in der Mesters Vig-Region (Scoresby Land, Nordostgrönland). Meddelelser om Grønland **72**(5), 26 pp.

13. Maps

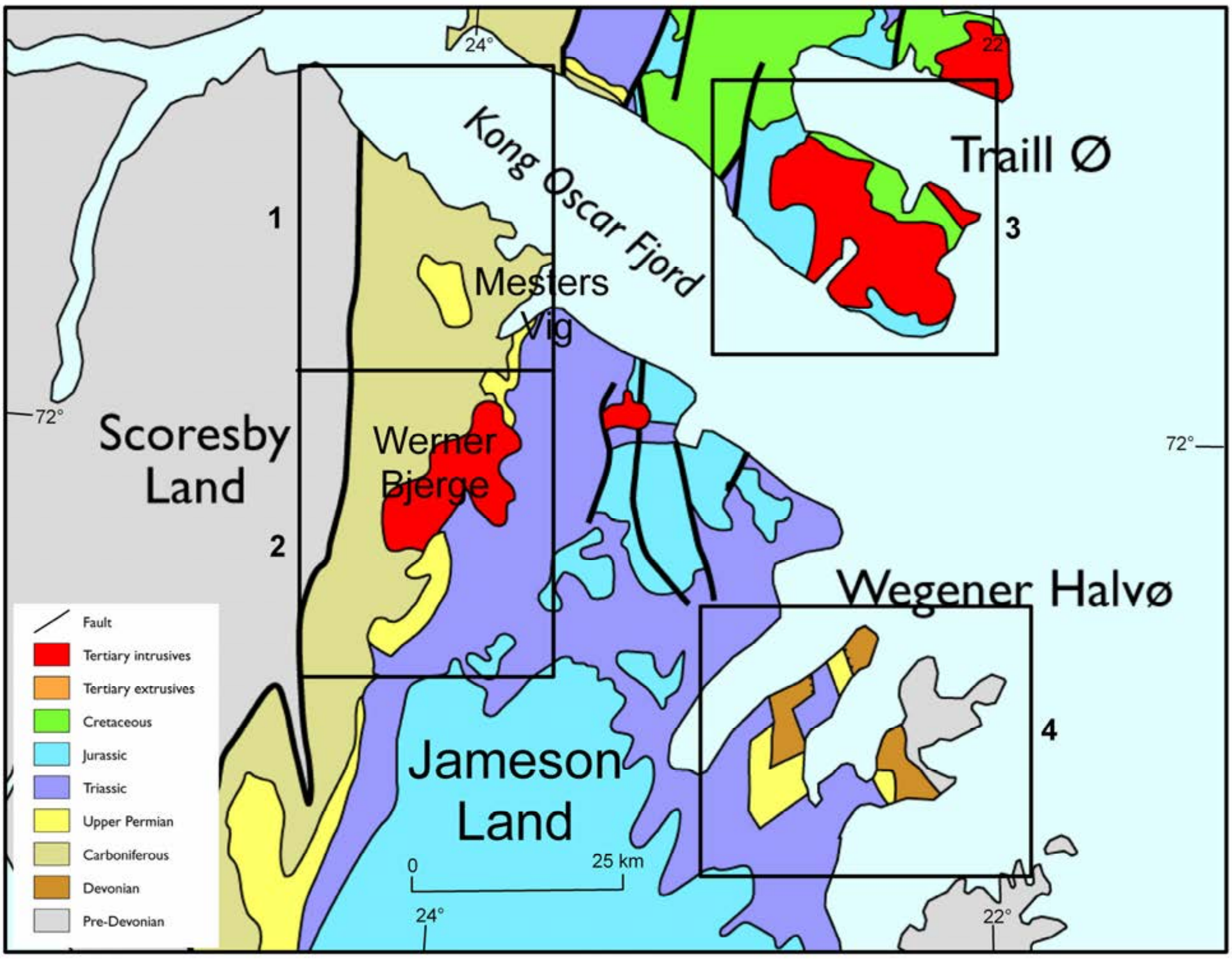

Map 1. *Simplified geological map of the greater Mesters Vig area. The numbered frames outline the four sub-areas investigated.*

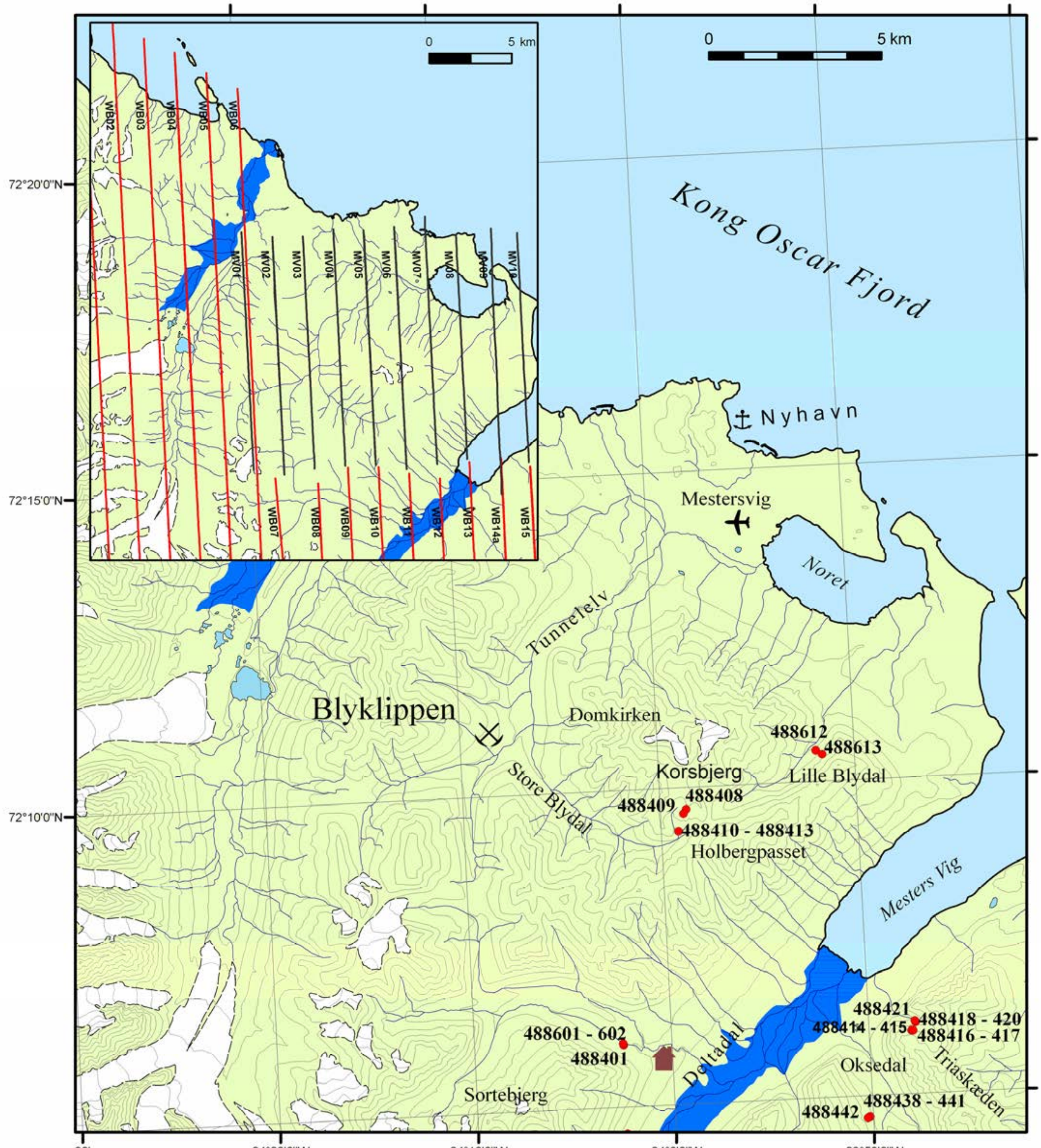

Map 2. *Locality and sample map of the Mesters Vig area. Hyperspectral flight lines are indicated on inset map.*

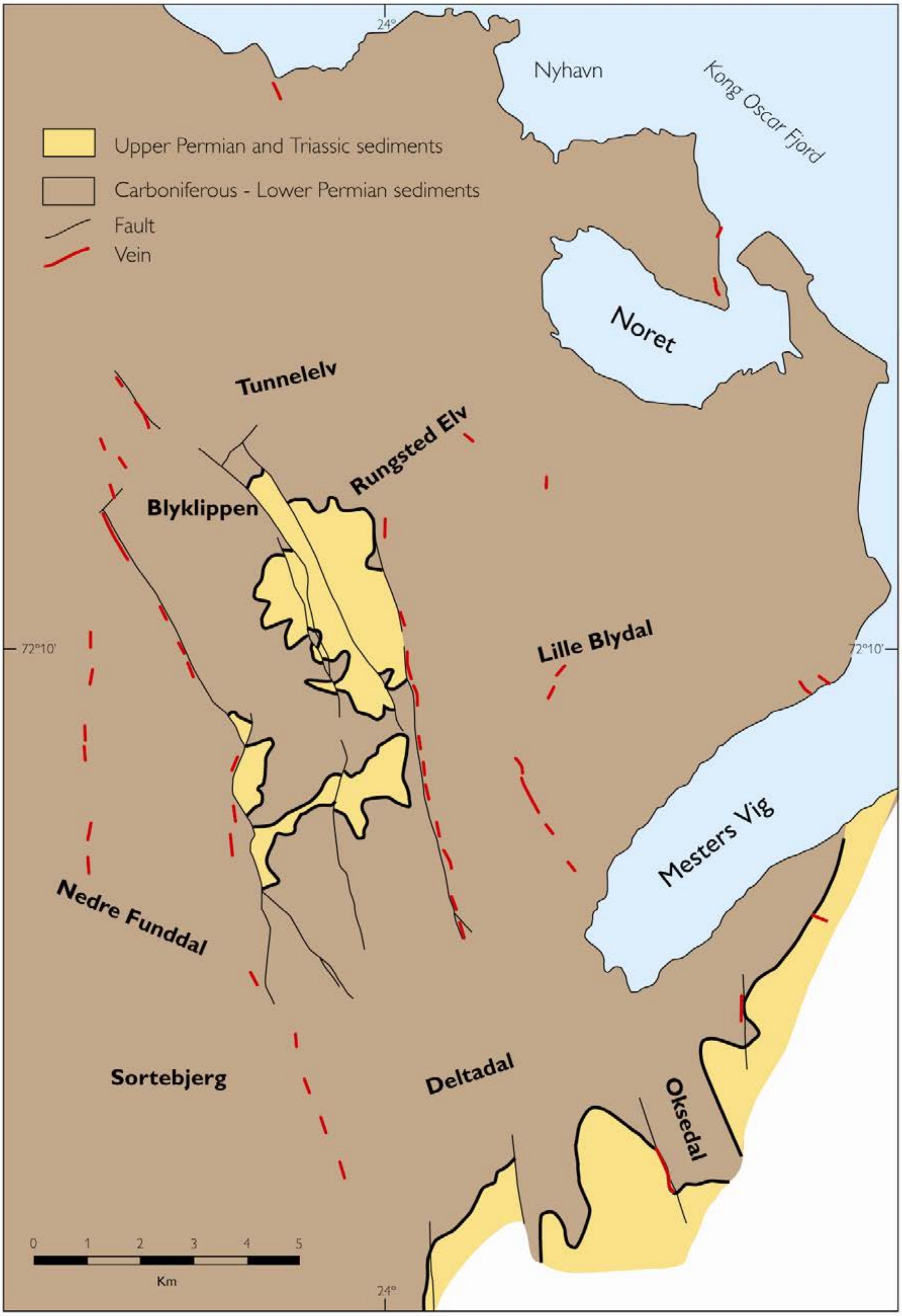

Map 3. *Simplified geological map of the Mesters Vig area showing the distribution of hydrothermale veins. Modified from Witzig (1954).*

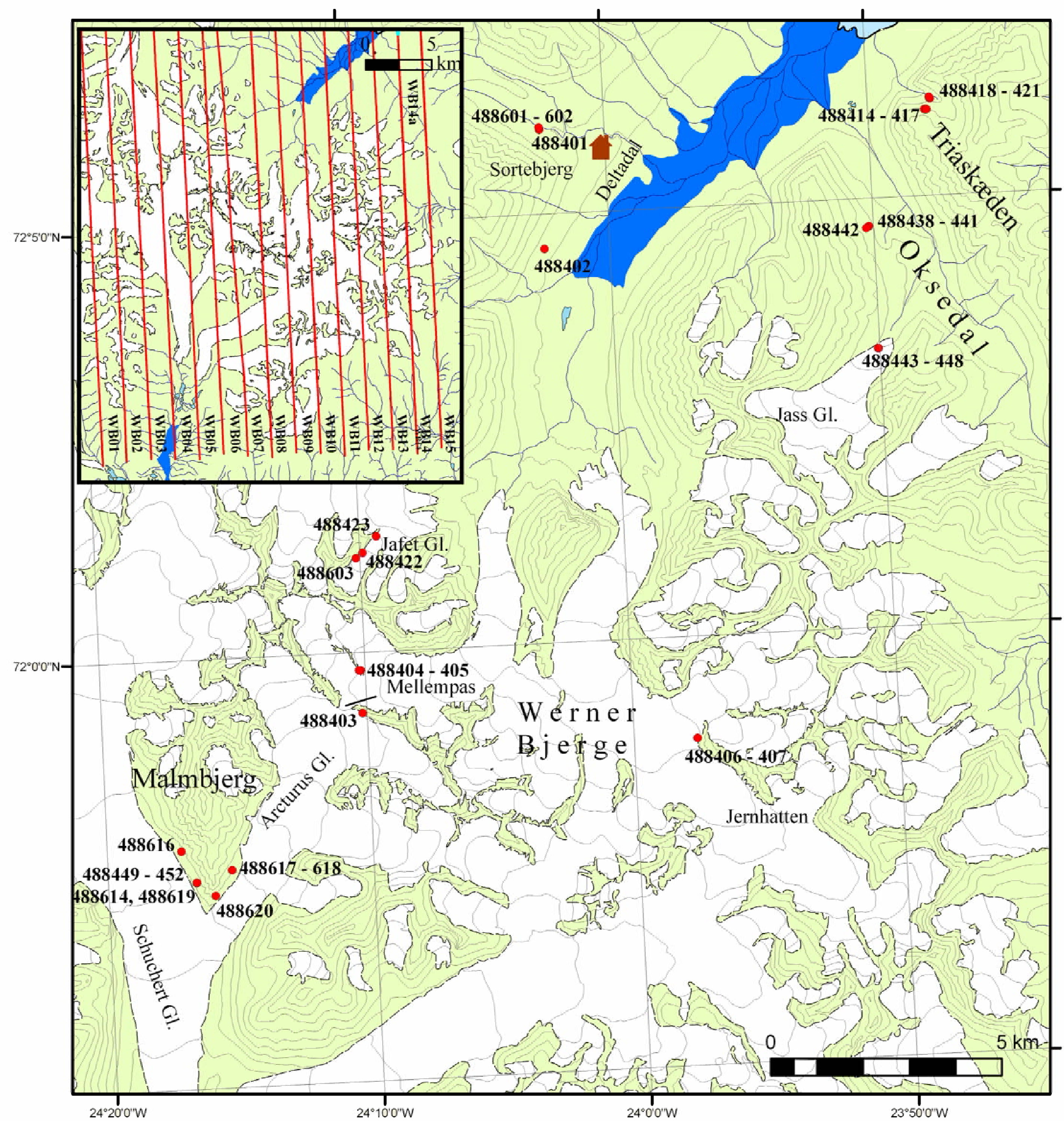

Map 4. *Locality and sample map of the Werner Bjerge. Hyperspectral flight lines are indicated on inset map.*

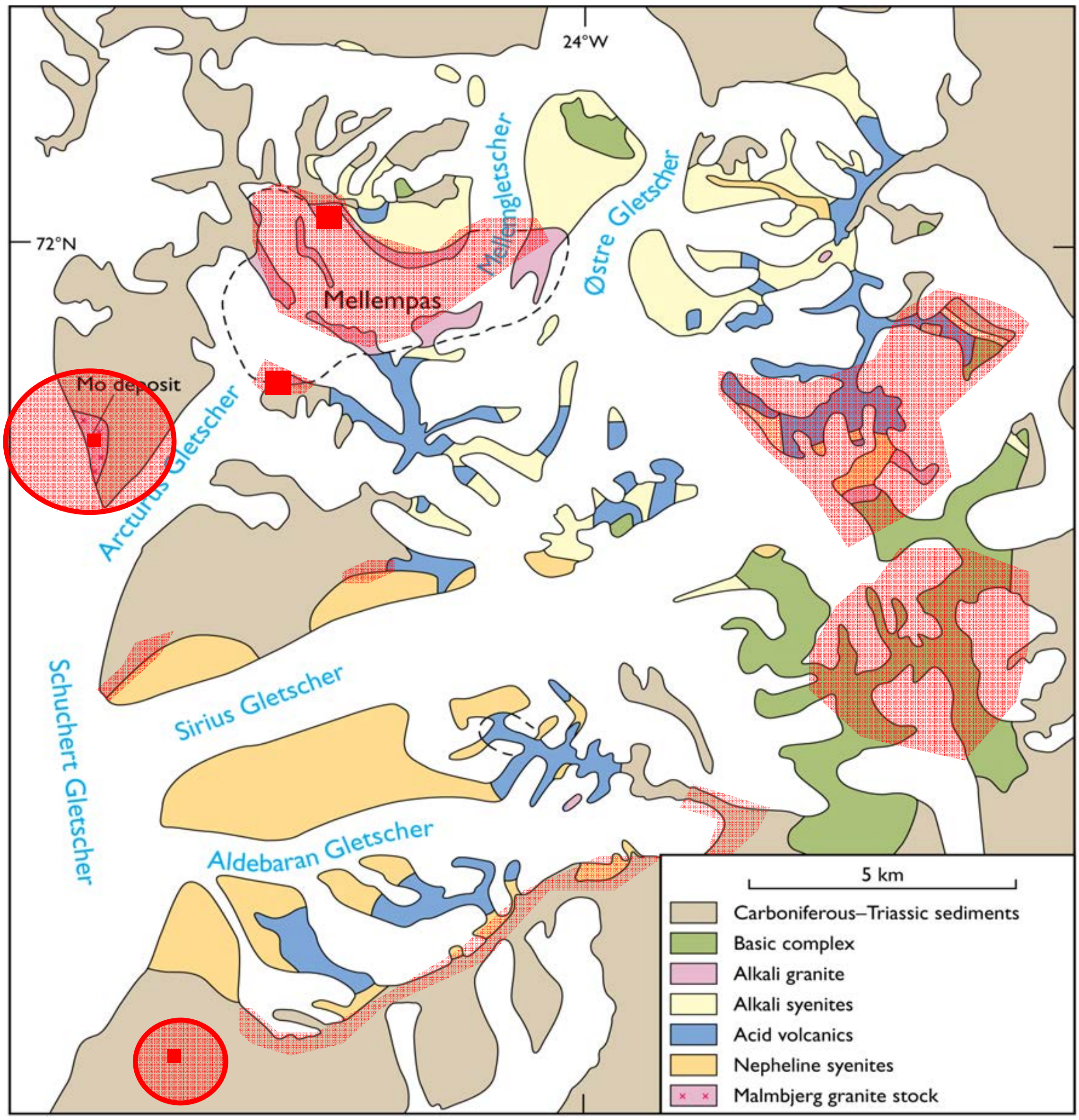

Map 5. *Geological map of the Werner Bjerge alkaline complex. Simplified after Bearth (1959). Major areas with hydrothermally altered and mineralised rocks mapped by the hyperspectral survey shown in pink. Encircled areas contain indications of high temperature potassic alteration. Red squares indicate greisensation.*

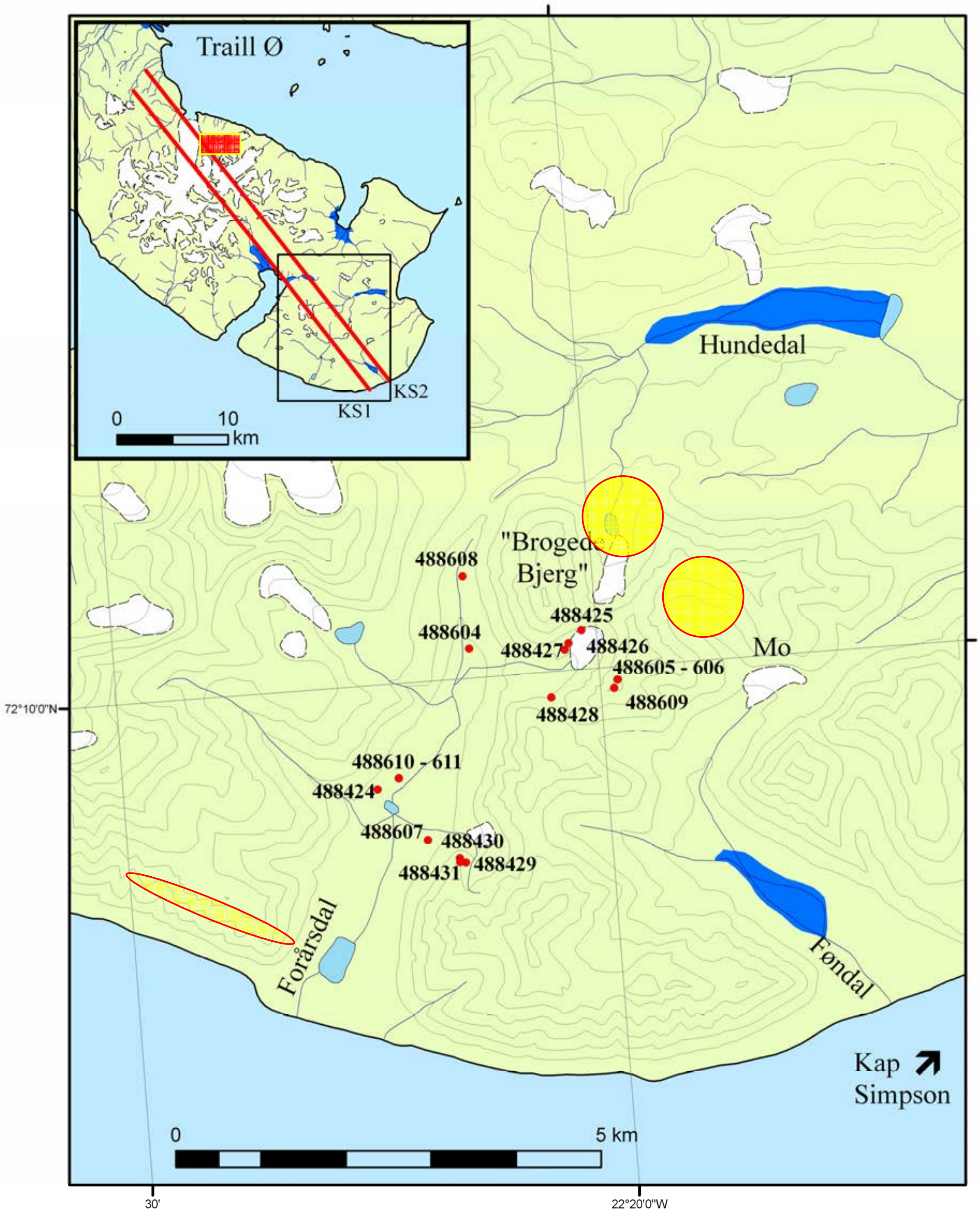

Map 6. *Locality and sample map of the Kap Simpson area. Hyperspectral flight lines are indicated on inset map. Mo: molybdenum anomaly. Areas with hyperspectral signature for high-temperature hydrothermal activity are indicated in yellow. Red area (east of Bredgletscher): greisen type alteration.*

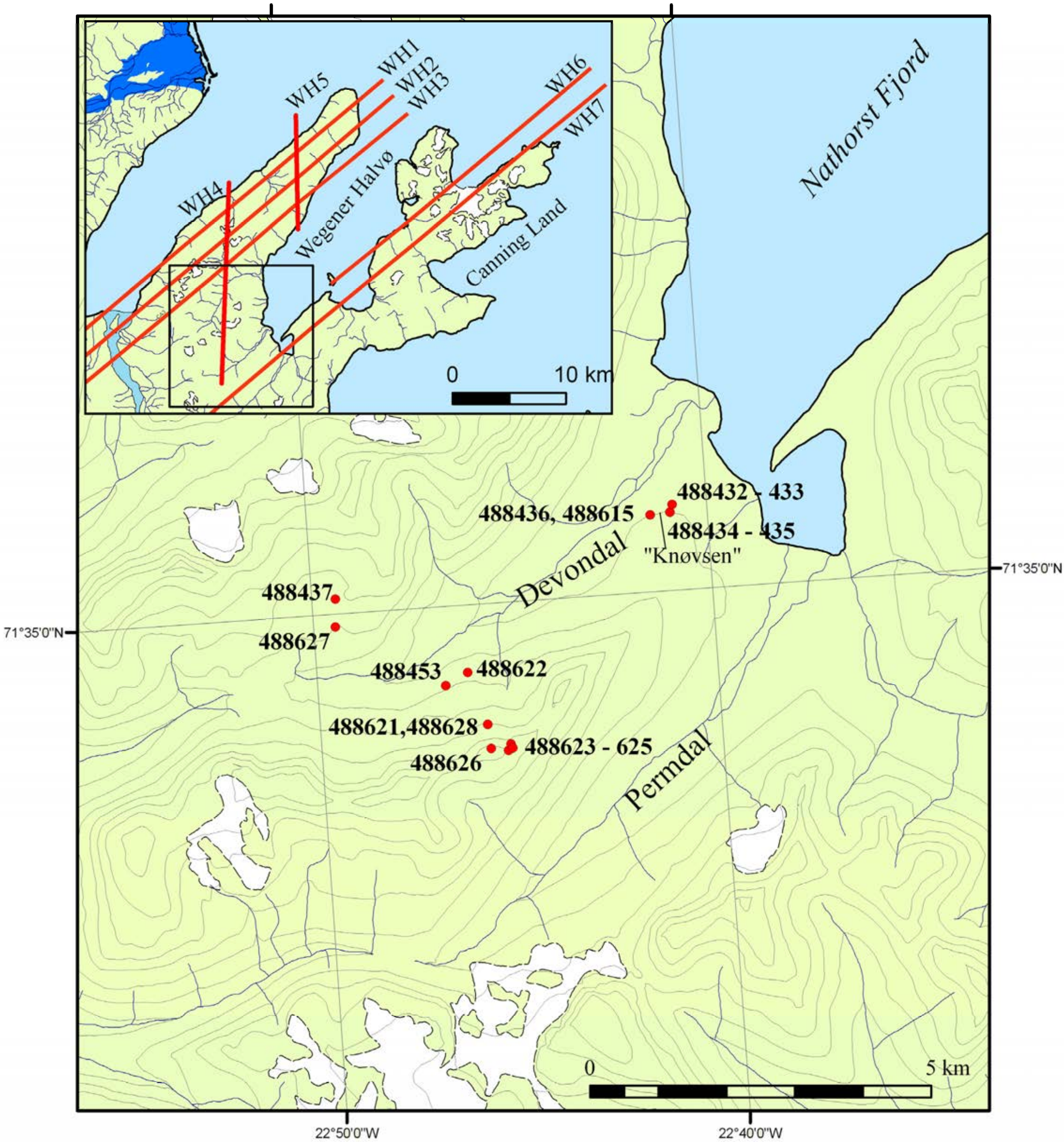

Map 7. *Locality and sample map of the Wegener Halvø area. Hyperspectral flight lines are indicated on inset map.*

14. Figures

Figure 1. *Open pit at the abandoned Blyklippen lead-zinc mine.*

Figure 2. *The Sortebjerg lead-zinc vein at Pings Elv Showing. View towards north-west.*

Figure 3. *Brown sphalerite and white quartz in bleached grey sandstone. The Sortebjerg vein at Pings Elv Showing.*

Figure 4. *Lens of massive galena covered by black oxidation minerals in the Sortebjerg vein, Sorte Hjørne Showing.*

Figure 5. *Zebra baryte at ‘Zebra Skar’ in Oksedal.*

Figure 6. *Zebra baryte at the ‘shoulder’ exposure in Triaskæden.*

Figure 7. *Finely banded zebra baryte from 'Zebra Skar', Oksedal, with 41.0% Ba (~69.7% baryte, 488441). Scale bar is 2 cm. Photo: Jakob Lautrup.*

Figure 8. *Coarsely banded zebra baryte from the main exposure in Triaskæden with 52.9% Ba (~89.9% baryte, 488414). Scale bar is 2 cm. Photo: Jakob Lautrup.*

Figure 9. *Laminated galena and chert from the 'shoulder' exposure in Triaskæden with 41.1% Pb and 1570 ppm Ag (488421). Scale bar is 2 cm. Photo: Jakob Lautrup.*

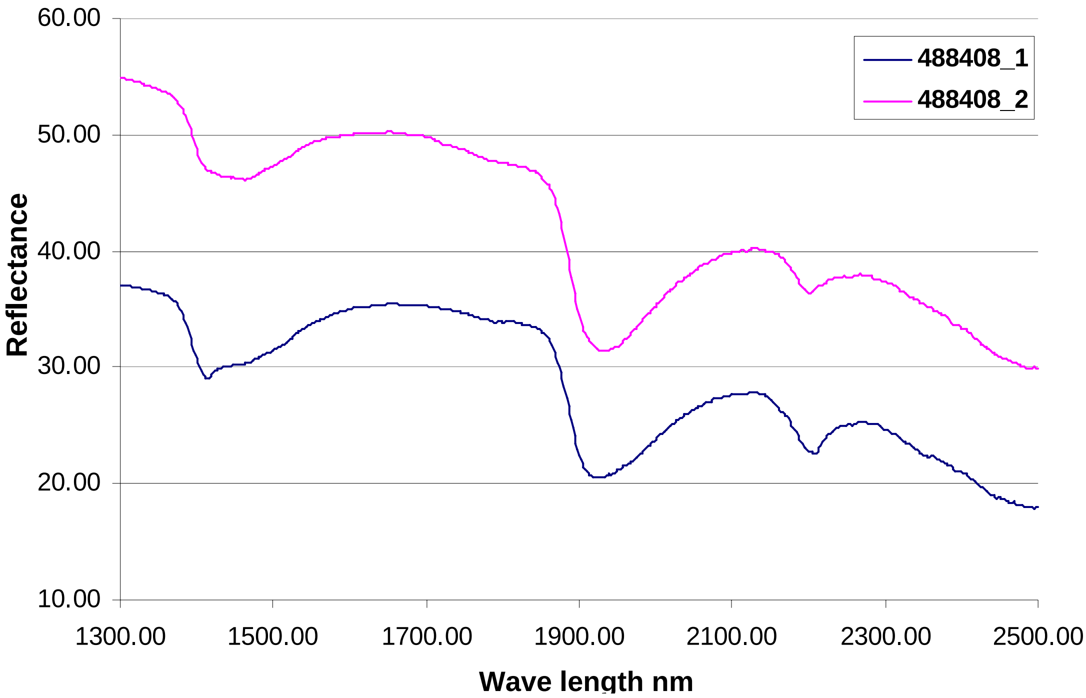

Figure 10. *PIMA spectra of baryte- and galena-bearing quartz vein from Holbergpasset (488408). The absorption features reflect minor amounts of kaolinite/halloysite.*

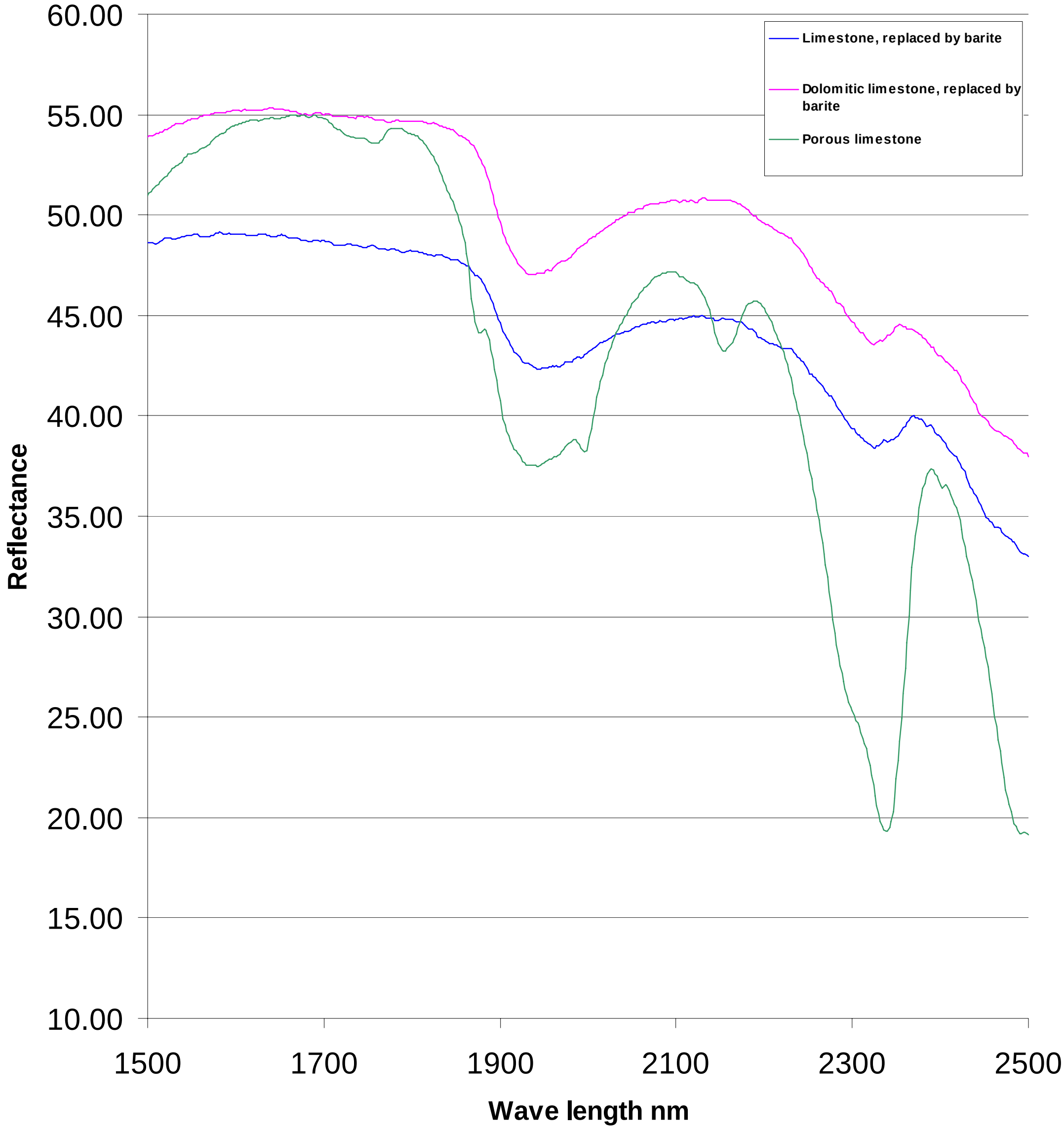

Figure 11. *PIMA spectra of Upper Permian limestone variably replaced by baryte, Oksedal.*

Figure 12. South-west view from Mellempas over Arcturus Gletscher towards Malmbjerg (central rust zone).

Figure 13. *The west side of Malmbjerg c. 500 m high exposing mineralised granite cupola and Schuchert adit portal; seen from InterMoly's camp on Schuchert Gletscher.*

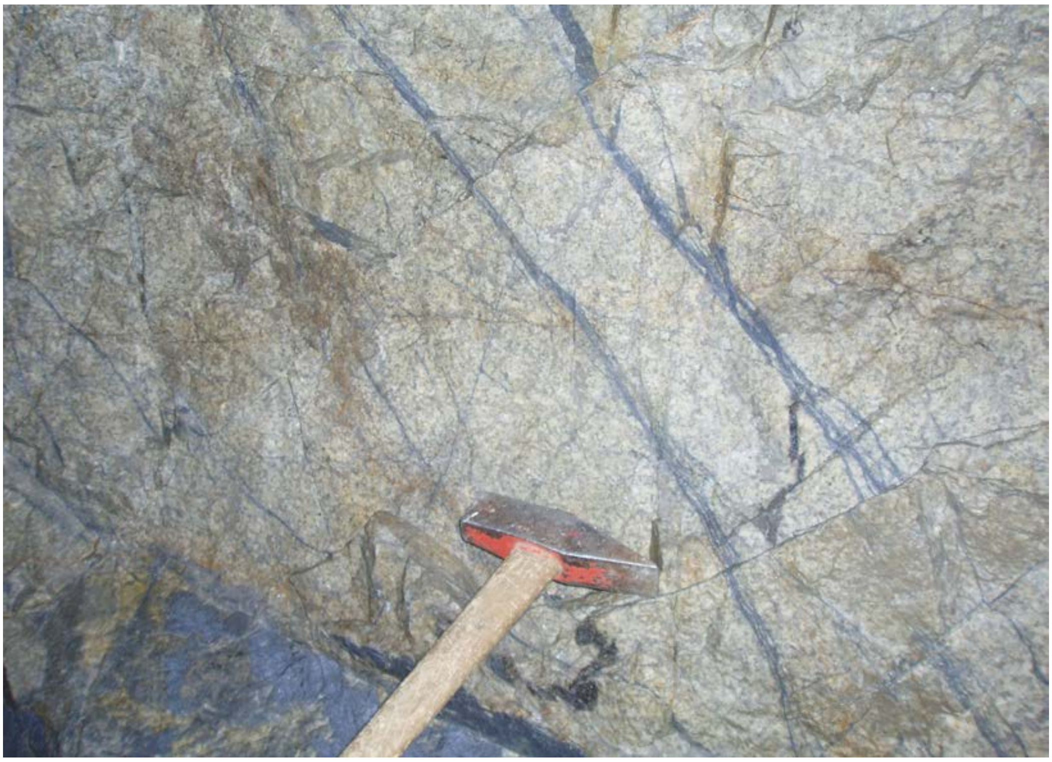

Figure 14. *Typical stockwork-type molybdenite mineralisation in the Schuchert adit.*

Figure 15. *Typical greisen-type mineralisation with wolframite (black crystals) in the Schuchert adit.*

Figure 16. *Drill core of Schuchert porphyry, Malmbjerg, with 0.12% Mo (488449). Scale bar is 2 cm. Photo: Jakob Lautrup.*

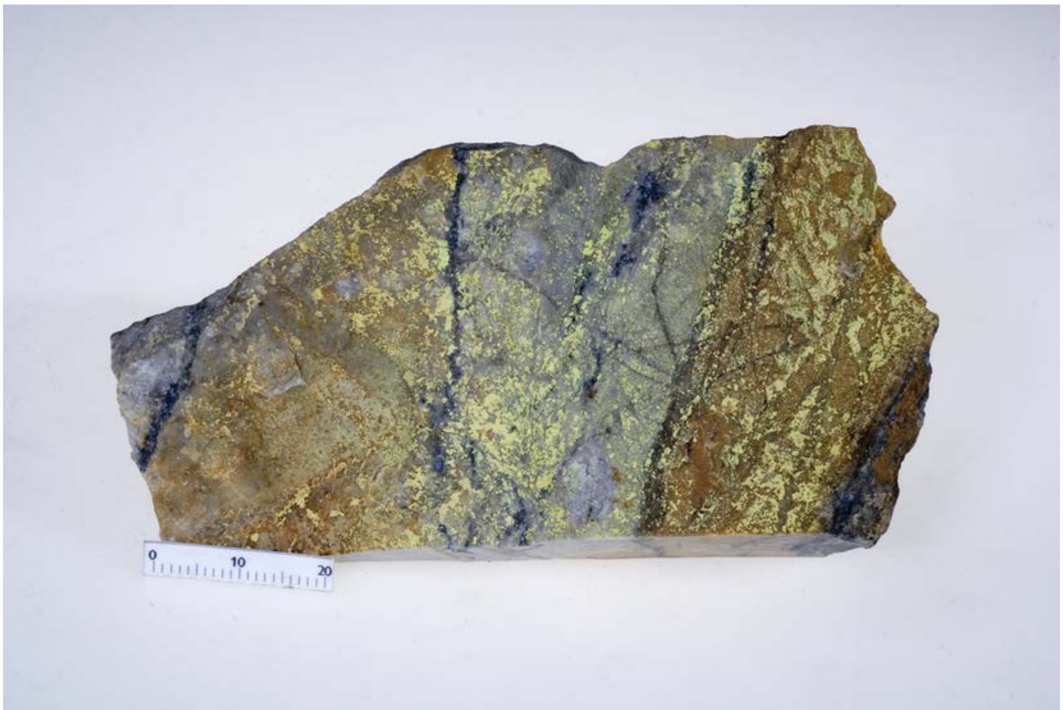

Figure 17. *Stockwork mineralisation with 0.97% Mo and coating of molybdic ochre from Malmbjerg (488619). Scale bar is 2 cm. Photo: Jakob Lautrup.*

Figure 18. *The ‘Mellemryg’ nunatak seen from Røde Mur, Mellempas. Relief is c. 800 m.*

Figure 19. *The north-western snout of Jernhatten exposing rusty volcanic breccias. Relief is c. 250 m.*

Figure 20. *Aerial view towards the south-west of Jafet Gletscher (central upper part of picture) with brownish Triassic sediments on the foreground hill top. Relief is c. 1000 m.*

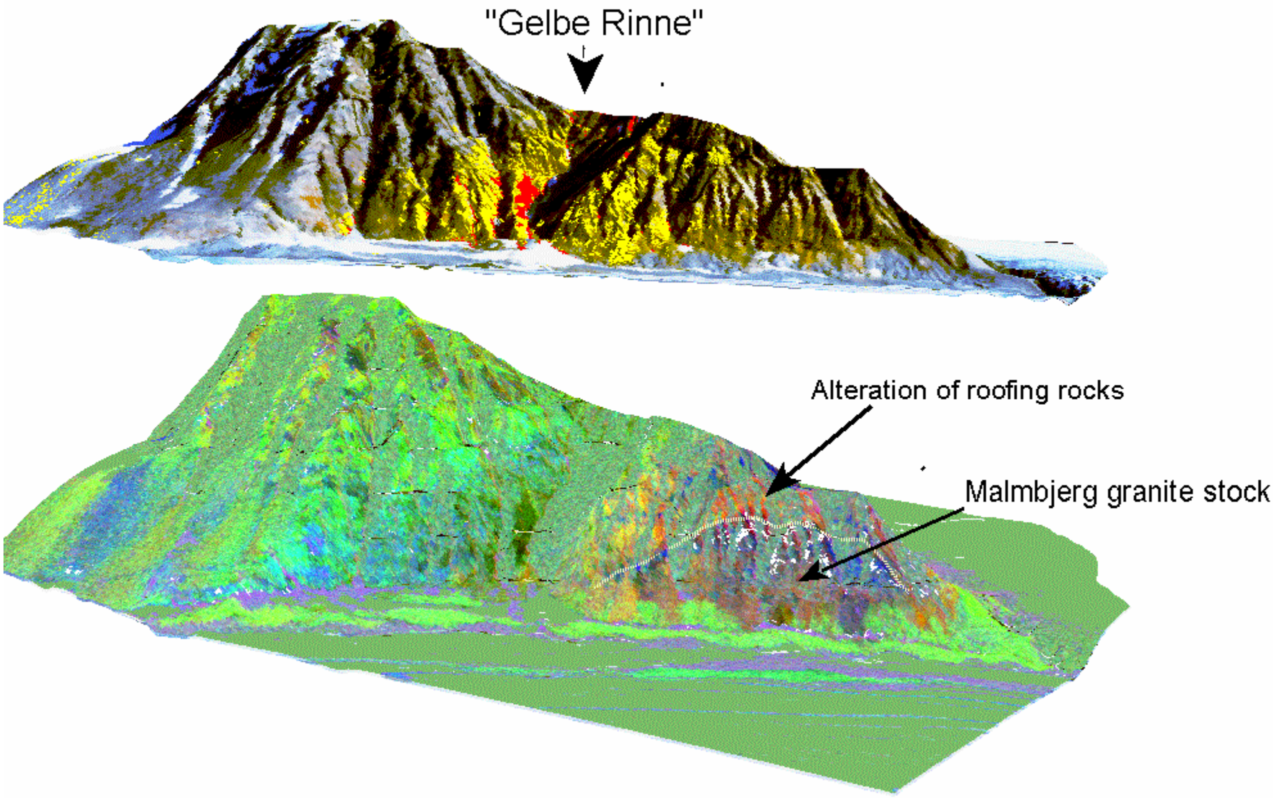

Figure 21. *Perspective view from the south-west of the Malmbjerg granite stock, no vertical exaggeration. DTM: resolution 50 x 50 m.* ***Top****: colour composite of HyMap bands 27(R), 18(G) and 4(B). The extensive alteration zone ('Gelbe Rinne') is characterised by the intensive formation of illite (yellow), jarosite (red) and hydrous Fe-oxides (not shown)* ***Bottom****: MNF-transformed HyMap SWIR-data. Note the intensive high temperature alteration of the roofing rocks (hues of yellow and orange). The Malmbjerg granite stock is outlined by blue and brown hues.*

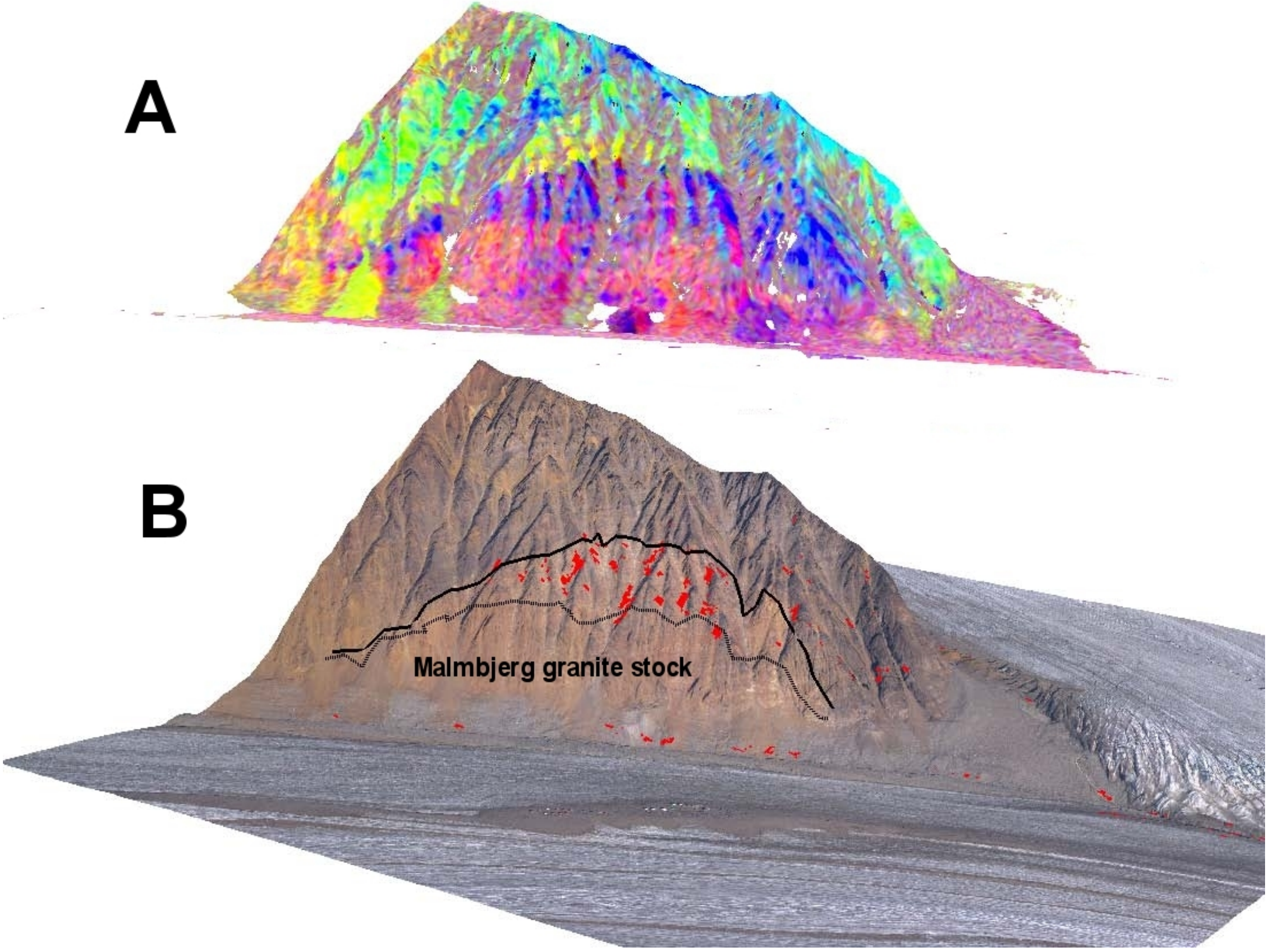

Figure 22. *Perspective view from the south-west of Malmbjerg granite stock, no vertical exaggeration. DTM: based on Lidar data from InterMoly (resampled to 1 x 1 m resolution). **A**. MNF-transformed SWIR data draped on the detailed DTM. Note the compositional zoning of the granite stock. **B**. Orthoscopic Lidar image draped on the detailed DTM. The pixels mapped as topaz/tourmaline-bearing greisen are shown with red. The geological boundaries of the granite stock are indicated.*

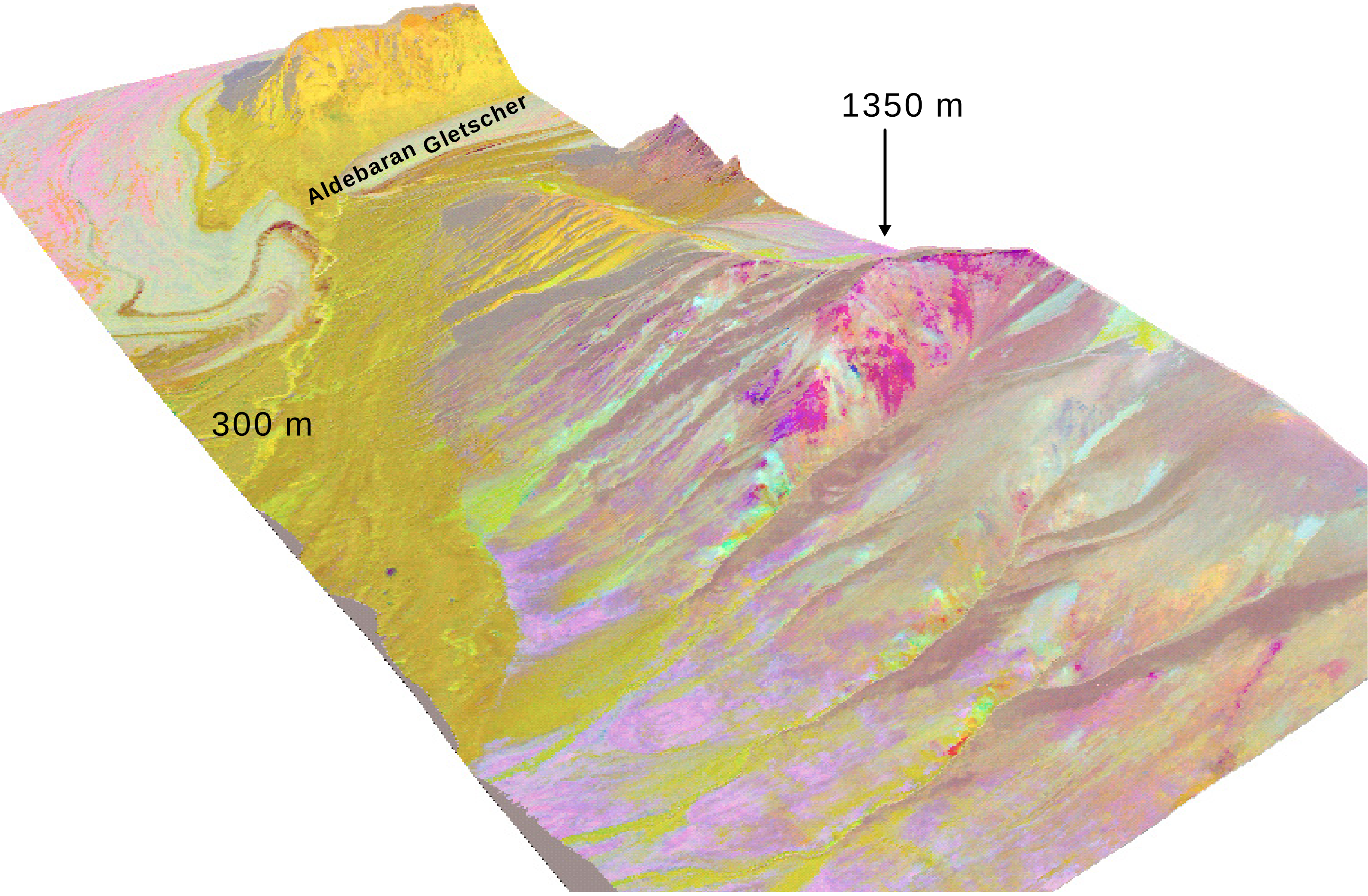

Figure 23. *Hydrothermally altered Carboniferous sandstone 3.5 km south of Aldebaran Gletcher. Perspective view from the south-west of MNF-transformed SWIR data. The area of hydrothermal alteration (iron oxides, muscovite/illite) is outlined by magenta and deep blue colours.*

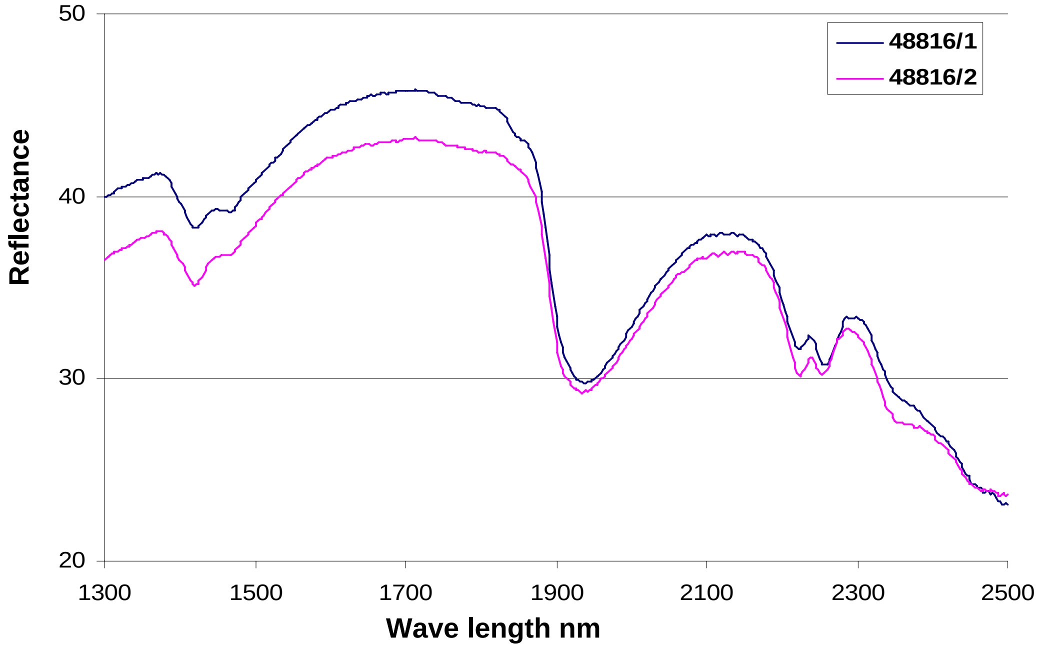

Figure 24. *PIMA spectra of altered rocks from 'Gelbe Rinne', Malmbjerg (488616). The material is partially altered to illite and jarosite.*

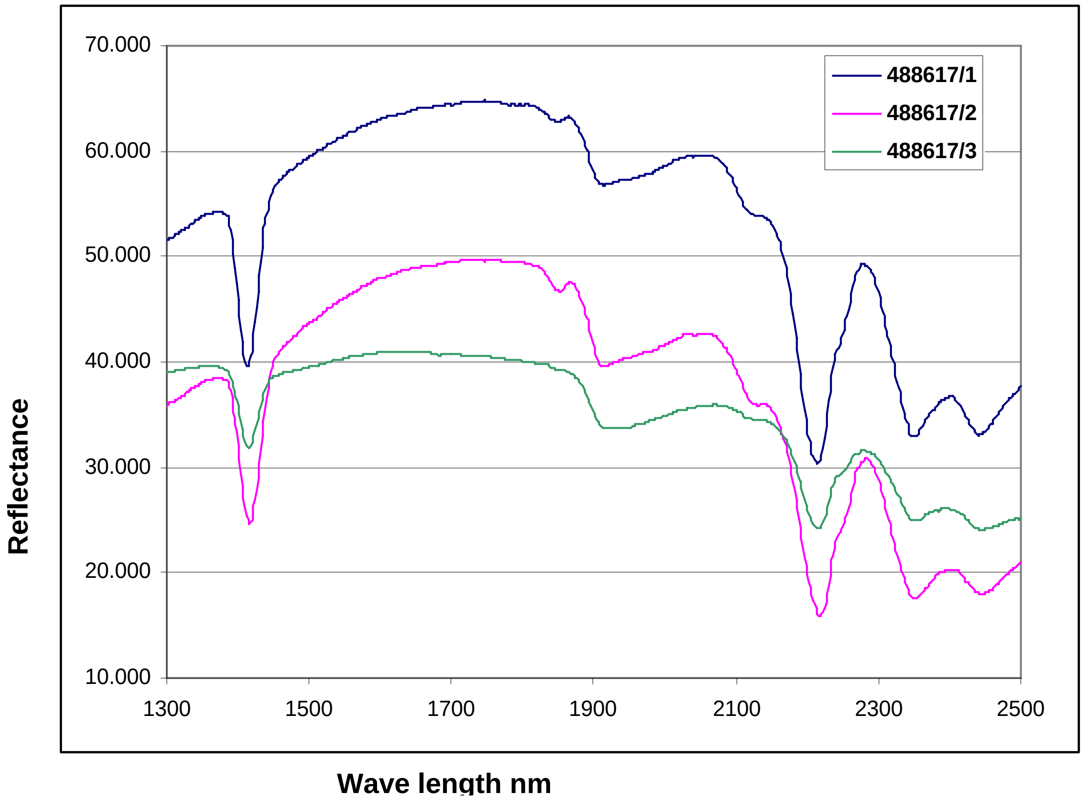

Figure 25. *PIMA spectra of altered material from 'Gelbe Rinne', Malmbjerg (488617). The material is predominantly illite with some nontronite and goethite.*

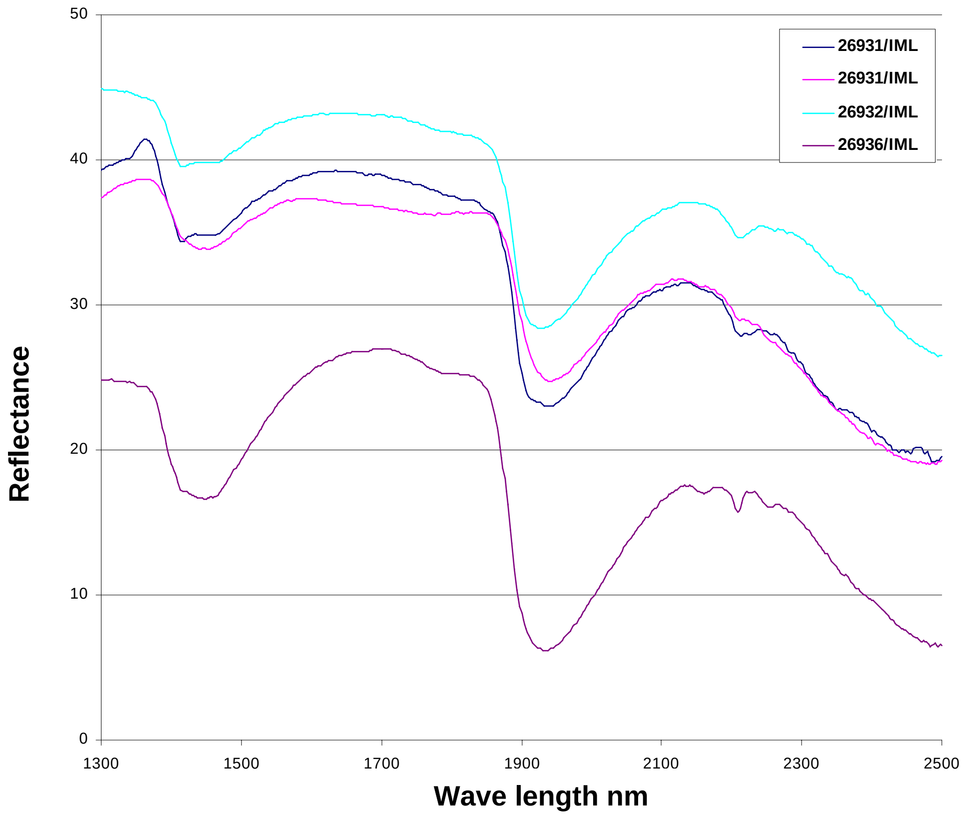

Figure 26. *PIMA spectra of granite from Malmbjerg. InterMoly samples.*

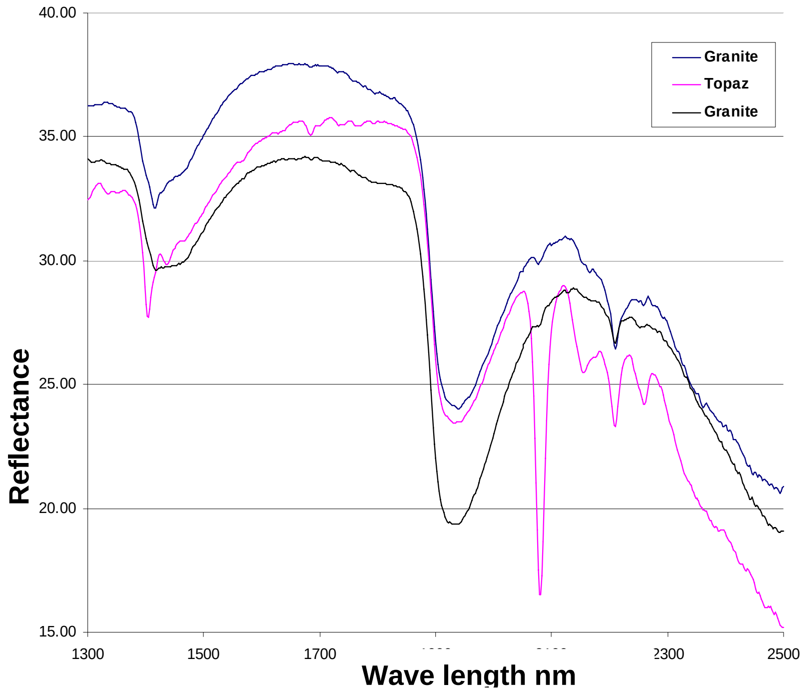

Figure 27. *PIMA spectra of a greisenized granite containing muscovite and topaz. Malmbjerg. InterMoly sample IML/26933.*

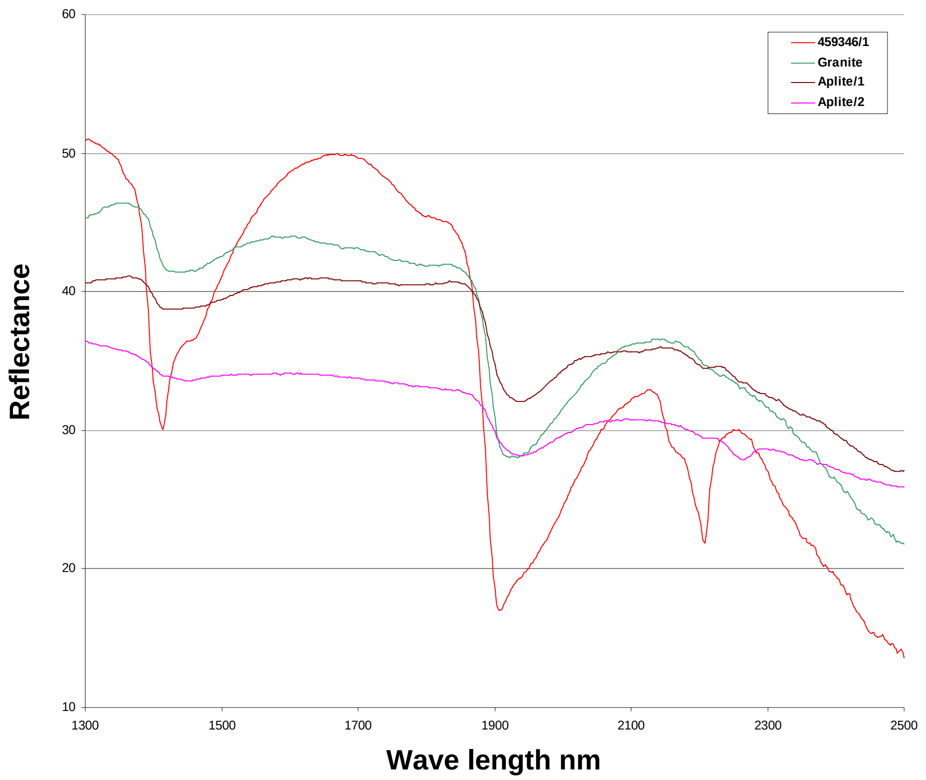

Figure 28. *PIMA spectra of granite, aplite and kaolin (459346) from Mellempas.*

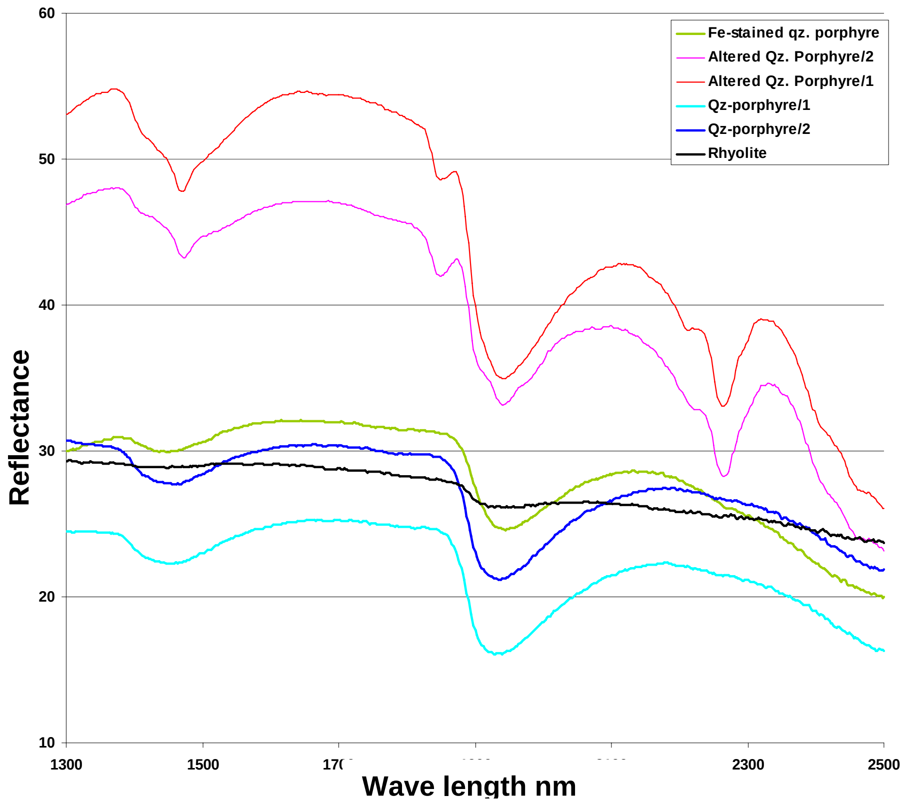

Figure 29. *PIMA spectra of quartz porphyry, rhyolite and hydrothermal alteration products (virtually pure jarosite with some illite) from Jernhatten.*

Figure 30. *Upper Føndal seen from the south-west with red-coloured molybdenum anomaly at the centre of the picture. Relief is c. 400 m.*

Figure 31. *The 'Brogede Bjerg' seen from the south. Relief is c. 500 m.*

Figure 32. *The west side of Forårsdal displaying rusty granite. Relief is c. 500 m.*

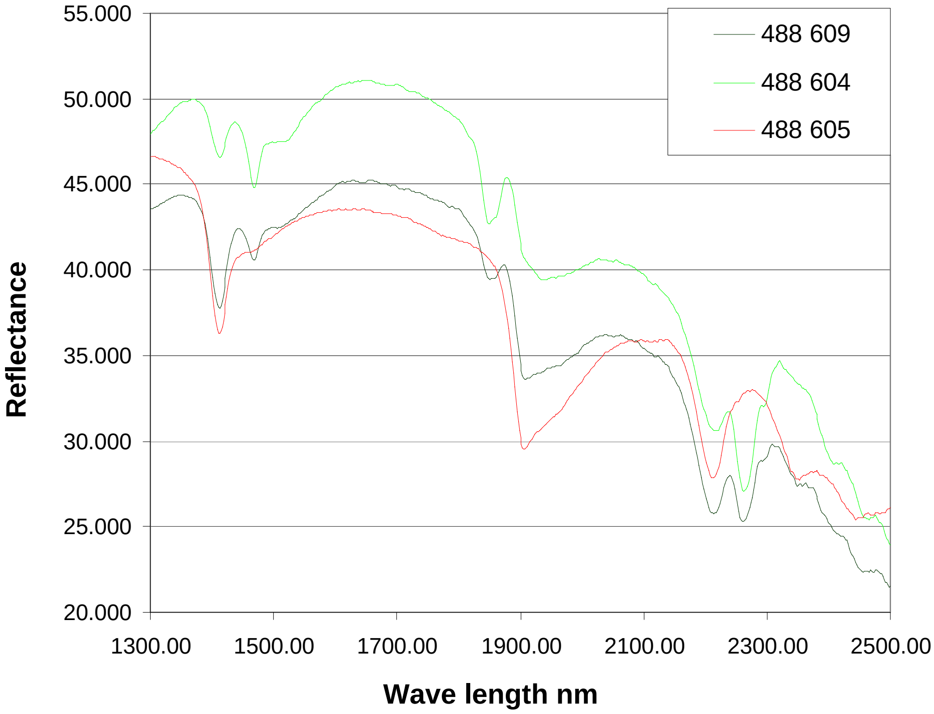

Figure 33. *PIMA spectra of altered rocks from Kap Simpson area.* ***488609****: breccia of altered acid volcanic rock, Forårsdal east. The altered material is a mixture of montmorillonite (44%), jarosite (35%) and illite (21%).* ***488604****: altered white-yellowish volcanic(?) rock rich in jarosite, Forårsdal.* ***488605****: intensively altered acid volcanic rock, Forårsdal east. The altered material is a mixture of montmorillonite (63%) and illite (37%).*

Figure 34. *View to the north-west of lower Devondal with malachite-stained Upper Permian sediments in the foreground ('Knøvsen') and Upper Permian sediments resting with an angular unconformity on Devonian sediments in the background. Relief is c. 900 m.*

Figure 35. *The south side of Devondal displaying Triassic sediments (red and green) resting on Upper Permian limestone (grey). Relief is c. 500 m.*

Figure 36. *Typical quartz-baryte-base-metal mineralisation in Wegener Halvø Formation limestone, southern Devondal.*

Figure 37. *Well-mineralised sample from Wegener Halvø Formation with 4.0% Cu, 88 ppm Ag, 0.7% As and 0.3% Zn (488436). Scale bar is 2 cm. Photo: Jakob Lautrup.*

Figure 38. *Mineralised red-bed sequence in the Triassic Klitdal Member, south Devondal.*

Figure 39. *Well-mineralised Klitdal Member arkose with 7.6% Cu, 14.3% Pb and 327 ppm Ag (488453). Scale bar is 2 cm. Photo: Jakob Lautrup.*

Figure 40. *White gypsum nodules in the Triassic Gipsdalen Formation, southern Devondal.*

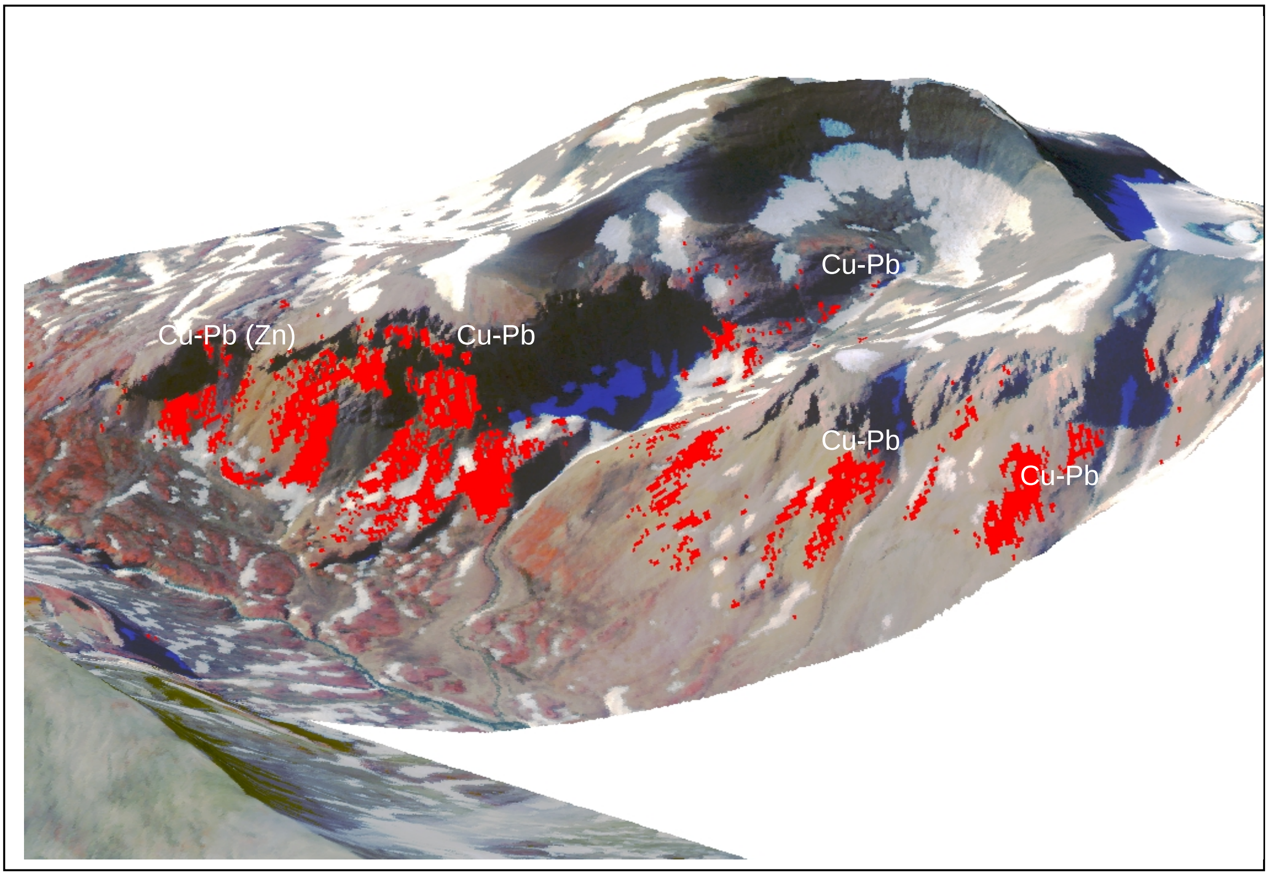

Figure 41. *Perspective view from the south-east of the north slope of Devondal showing dolomitic alteration (red) of the Upper Permian limestone. The known occurrences of Cu-Pb-Zn mineralisation are indicated. Background image colour composite of HyMap bands 27(R), 18(G) and 4(B). No vertical exaggeration.*

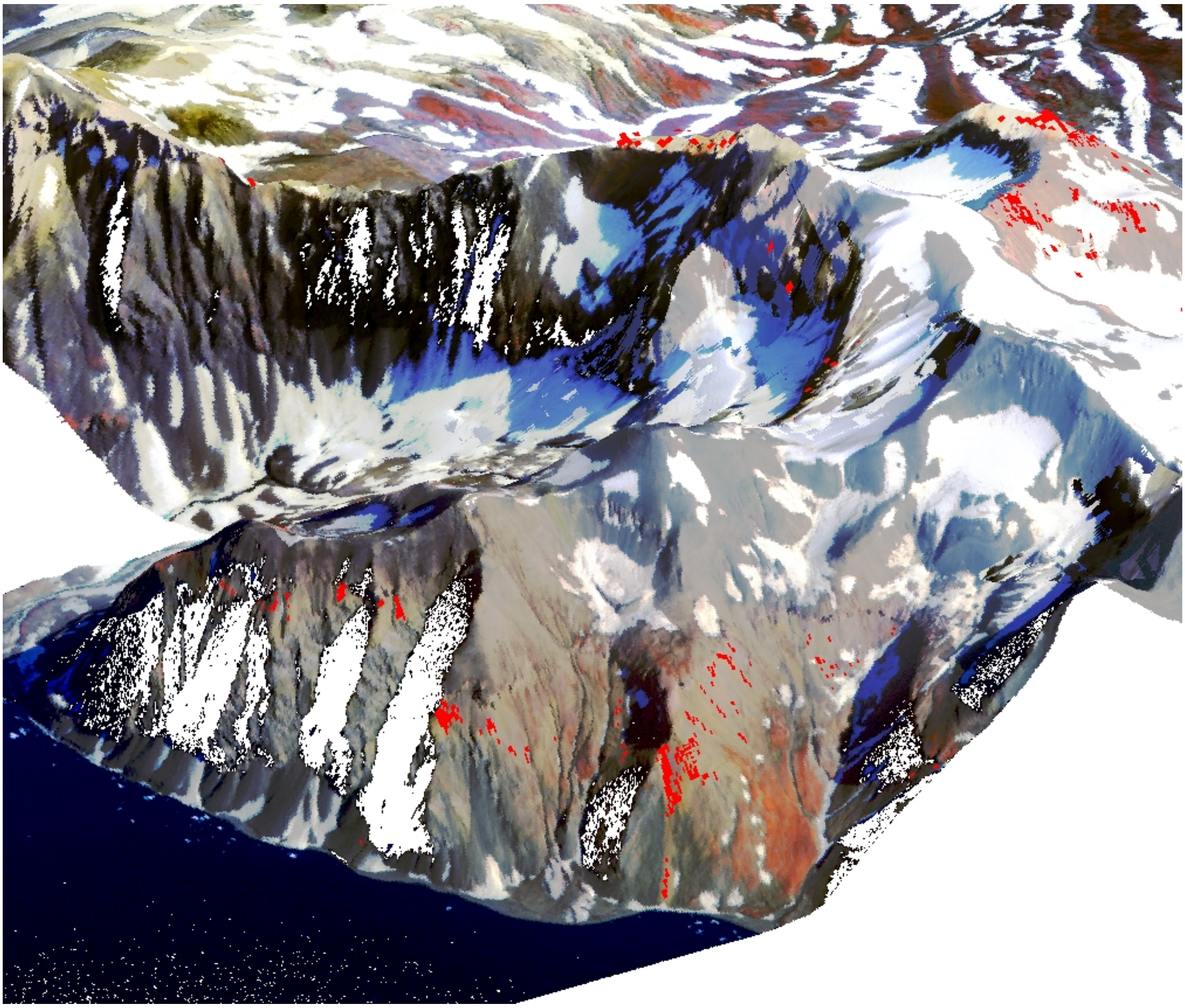

Figure 42. *Perspective view from the north of central Wegener Halvø (Vimmelskaftet) showing dolomitic alteration (red) of the Upper Permian limestone. Background image colour composite of HyMap bands 27(R), 18(G) and 4(B). No vertical exaggeration.*

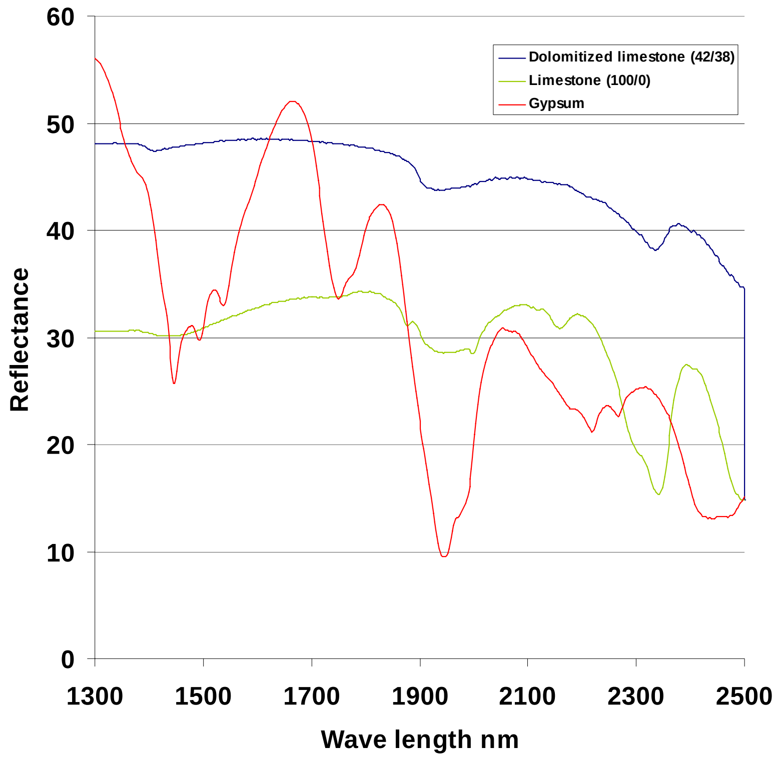

Figure 43. *PIMA spectra of Upper Permian carbonate rocks at 'Knøvsen' and spectrum of a gypsum nodule (100% gypsum) from the Triassic Gipsdalen Formation, southern Devondal (Figure 40). The carbonate rock hosting mineralisation (Figure 34) is dolomitized (calcite/dolomite ratio 42/38). The surrounding limestone is calcitic.*

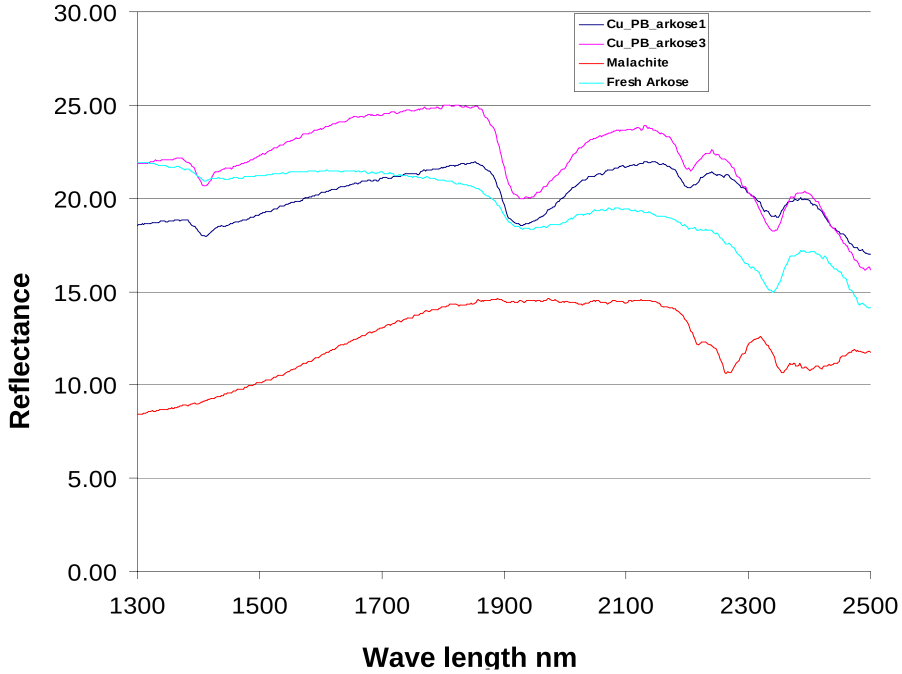

Figure 44. *PIMA spectra of the mineralised red-bed sequence in the Triassic Klitdal Member. The Cu-Pb mineralised arkose contains calcite.*

15. Tables

Table 1. Rock sample list

GGU no.	Latitude	Longitude	Alt. m	Area	Type	Field description
488401	72.1000	-24.0407	213	1	o	Banded qtz.-sph. vein
488402	72.0768	-24.0410	146	2	b	Aplite with mo.
488403	71.9884	-24.1693	1186	2	o	Miarolitic aplite with mo.
488404	71.9967	-24.1693	966	2	b	Aplite with qtz.-py.-mo. veinlets
488405	71.9968	-24.1703	950	2	o	Aplite with qtz.-py. veinlets.
488406	71.9805	-23.9602	703	2	b	Breccia (agglomerate?) with py.
488407	71.9805	-23.9602	703	2	b	Fragmental, siliceous rock with py.
488408	72.1614	-23.9778	885	1	b	Vqz. with ba. and ga.
488409	72.1603	-23.9803	863	1	o	Upper Permian porouse limestone
488410	72.1557	-23.9853	684	1	o	Barytised Upper Permian limestone
488411	72.1557	-23.9853	684	1	o	Barytised Upper Permian limestone
488412	72.1557	-23.9853	684	1	o	Barytised Upper Permian limestone
488413	72.1557	-23.9853	684	1	o	Barytised Upper Permian limestone
488414	72.1002	-23.7973	495	1	b	Zebra ba.
488415	72.1002	-23.7973	495	1	b	Barytised limestone, trace ga.
488416	72.1002	-23.7961	501	1	b	Ba. with trace ga.
488417	72.1002	-23.7961	501	1	b	Zebra ba.
488418	72.1023	-23.7935	277	1	b	Barytised limestone with ga.
488419	72.1023	-23.7935	277	1	b	Barytised limestone with ga.
488420	72.1023	-23.7935	277	1	b	Barytised limestone with ga.
488421	72.1026	-23.7941	278	1	o	Silicified limestone with ga.
488422	72.0195	-24.1647	942	2	b	Skarnoid rock with py.+ mag.
488423	72.0226	-24.1556	811	2	b	Biotite-rich dyke rock with mag.+ py.
488424	72.1557	-22.4125	76	3	b	Granite with py.
488425	72.1709	-22.3384	357	3	b	Felsic rock with py.
488426	72.1696	-22.3431	325	3	b	Volcanic breccia with py.
488427	72.1690	-22.3446	339	3	b	Volcanic breccia with trace py.
488428	72.1640	-22.3504	291	3	b	Metasediment with semi-massive py.
488429	72.1473	-22.3841	166	3	b	Aplite with vein fluorite and trace py.
488430	72.1478	-22.3861	264	3	b	Granite with vein fluorite
488431	72.1474	-22.3861	294	3	oc	Felsite with fluorite lenses and veinlets
488432	71.5937	-22.6819	116	4	o	Vqz. with cpy. and ga.
488433	71.5937	-22.6819	116	4	o	Vqz. with ga. and sph.
488434	71.5948	-22.6808	96	4	b	Breccia with vqz., ba., cpy. and ga.
488435	71.5948	-22.6808	96	4	b	Vqz. with cpy. and ga.
488436	71.5936	-22.6902	171	4	o	Ba.-qtz. vein with tet.
488437	71.5854	-22.8233	476	4	b	Upper permian limestone with tet.
488438	72.0781	-23.8360	281	1	o	Zebra ba. with ga.
488439	72.0781	-23.8360	281	1	o	Zebra ba. with minor ga.
488440	72.0781	-23.8360	281	1	o	Zebra ba. and limestone with ga.
488441	72.0781	-23.8360	281	1	o	Zebra ba. with trace ga.
488442	72.0777	-23.8378	229	1	o	Barytised limestone with ga.
488443	72.0543	-23.8341	395	2	b	Granite with py.
488444	72.0543	-23.8341	395	2	b	Syenite with chlorite and py.

Table 1. Rock sample list

GGU no.	Latitude	Longitude	Alt. m	Area	Type	Field description
488445	72.0543	-23.8341	395	2	b	Granite with py.
488446	72.0543	-23.8341	395	2	b	Felsite with py.
488447	72.0543	-23.8341	395	2	b	Syenite with py.-veinlet
488448	72.0543	-23.8341	395	2	b	Calcite-cemented breccia with py., ga., and sph.
488449	71.9570	-24.2780	720	2	d	Schuchert porphyry with mo.
488450	71.9570	-24.2780	720	2	d	Greisen with wol., mo. and py.
488451	71.9570	-24.2780	720	2	d	Perthit granite with mo.
488452	71.9570	-24.2780	720	2	d	Granite
488453	71.5730	-22.7800	330	4	b	Arkose with disseminated cc. and ga.
488601	72.10043	-24.04097	167	1	o	Coarse grained sph. from qtz-ba vein
488602	72.10043	-24.04097	167	1	o	Vqz. with Fe-carbonate(?)
488603	72.01857	-24.16896	972	2	o	Intermediate-mafic sill with disseminated py.
488604	72.16987	-22.3774	50	3	b	White-yellowish altered syenite/trachyte
488605	72.16539	-22.32724	624	3	o	Kaolinized acid volcanic rock
488606	72.16539	-22.32724	624	3	o	Kaolinized acid volcanic rock
488607	72.14994	-22.39658	34	3	o	Altered acid volcanic rock
488608	72.17752	-22.37773	144	3	b	Sheared acid volcanic rock
488609	72.16452	-22.32857	616	3	o	Breccia of altered acid volcanic rock
488610	72.15674	-22.40494	32	3	o	Qtz.-rich pyritiferous rock
488611	72.15674	-22.40494	32	3	o	Rhyolite, type sample
488612	72.17518	-23.86563	339	1	b	Vqz. with ga.
488613	72.17412	-23.86036	424	1	o	Vqz. with sph. and ga.
488614	71.9570	-24.2780	720	2	o	0.4 m wide vertical clay zone.
488615	71.5936	-22.6902	170	4	oc	Upper Permian limestone, samples 1-10
488616	71.96312	-24.28679	754	2	o	Hydrothermally altered sandstone (?)
488617	71.95911	-24.25561	762	2	o	Hydrothermally altered sandstone (illite rock)
488618	71.95911	-24.25561	762	2	b	Sandstone with greisen (qtz.+wol.)
488619	71.9570	-24.2780	720	2	b	Mo. stockwork + molybdenun ochra (?)
488620	71.95425	-24.26654	730	2	o	Sandstone
488621	71.56753	-22.7638	534	4	o	Ga. mineralised coarse sandstone
488622	71.57454	-22.77061	284	4	oc	Cu-mineralised carbonate reef with ba.+qtz.
488623	71.56395	-22.75595	703	4	o	Dolomite
488624	71.56476	-22.75472	576	4	o	Myalina sandstone
488625	71.56421	-22.7541	644	4	o	Gypsum
488626	71.56436	-22.76307	795	4	o	Red mudstone
488627	71.58174	-22.82416	382	4	o	Carbonate reef
488628	71.56753	-22.7638	534	4	o	Cc. mineralised coarse sandstone

Table 1. Rock sample list

Abbreviations

d	=	drill core
o	=	sample from outcrop
oc	=	composite sample from outcrop
b	=	boulder or scree sample
c1.0	=	chip sample over 1.0 m
ba.	=	baryte
cc.	=	chalcocite
cpy.	=	chalcopyrite
ga.	=	galena
hem.	=	hematite
mag.	=	magnetite
mal.	=	malachite
mo.	=	molybdenite
py.	=	pyrite
pyrrh.	=	pyrrhotite
sph.	=	sphalerite
tet.	=	tetrahedtite-tennantite
vqz.	=	vein quartz
wol.	=	wolframite

Table 2. Analytical results

Element	Detection limit		Analytical method	Element	Detection limit		Analytical method
Ag	0.3	ppm	ICP	Mo	1	ppm	ICP
Au	2	ppb	INAA	Na	0.01	pct	INAA
Al	0.01	pct	INAA	Nd	5	ppm	INAA
As	0.5	ppm	INAA	Ni	1	ppm	ICP
Ba	50	ppm	INAA	P	0.001	pct	ICP
Be	1	ppm	ICP	Pb	3	ppm	ICP
Bi	2	ppm	ICP	Pb >0.5%	30	ppm	ICP-OES
Br	0.5	ppm	INAA	Rb	15	ppm	INAA
Ca	0.01	pct	ICP	S	0.01	pct	ICP
Cd	0.3	ppm	ICP	Sb	0.1	ppm	INAA
Ce	3	ppm	INAA	Sc	0.1	ppm	INAA
Co	1	ppm	INAA	Se	3	ppm	INAA
Cr	2	ppm	INAA	Sm	0.1	ppm	INAA
Cs	1	ppm	INAA	Sn	0.01	pct	INAA
Cu	1	ppm	ICP	Sr	1	ppm	ICP
Cu >1%	10	ppm	ICP-OES	Ta	0.5	ppm	INAA
Eu	0.2	ppm	INAA	Tb	0.5	ppm	INAA
Fe	0.01	pct	INAA	Th	0.2	ppm	INAA
Hf	1	ppm	INAA	Ti	0.01	pct	ICP
Hg	1	ppm	INAA	U	0.5	ppm	INAA
Ir	5	ppb	INAA	V	2	ppm	ICP
K	0.01	pct	ICP	W	1	ppm	INAA
La	0.5	ppm	INAA	Y	1	ppm	ICP
Lu	0.05	ppm	INAA	Yb	0.2	ppm	INAA
Mg	0.01	pct	ICP	Zn	1	ppm	ICP
Mn	1	ppm	ICP	Zn >10%	10	ppm	ICP-OES

Analysis by Activation Laboratories Ltd., Ontario, Canada.

Analytical methods:

INAA:	Instrumental neutron activation
ICP:	Inductively coupled plasma emission spectrometry
OES;	Optical emission spectrometry
Assay:	Cu>1%, Pb>0.5%, Zn>10% (total assays)

Table 2. Analytical results

GGU no.	Cu ppm	Pb ppm	Zn ppm	Ag ppm	Cd ppm	Bi ppm	Sb ppm	Hg ppm	Fe pct	S pct
488401	468	51	217000	< 0.3	1090.0	4	31.9	25	0.53	12.500
488402	62	< 3	374	< 0.3	0.7	< 2	0.3	< 1	3.08	0.570
488403	11	9	207	< 0.3	0.7	< 2	0.4	< 1	0.62	0.100
488404	5	3790	295	< 0.3	1.6	< 2	2.4	< 1	0.91	0.780
488405	4	178	398	< 0.3	1.4	< 2	0.8	< 1	1.30	1.480
488406	15	< 3	130	< 0.3	< 0.3	< 2	< 0.1	< 1	2.72	0.770
488407	4	< 3	130	< 0.3	< 0.3	< 2	0.2	< 1	1.55	2.390
488408	113	21800	< 1	< 0.3	< 0.3	< 2	3.4	< 1	0.13	0.510
488409	4	74	< 1	< 0.3	< 0.3	< 2	< 0.1	< 1	0.11	0.130
488410	7	< 3	198	< 0.3	1.5	< 2	2.1	< 1	0.50	0.160
488411	22	166	499	< 0.3	4.0	< 2	4.8	< 1	2.61	0.550
488412	63	314	465	< 0.3	6.5	< 2	10.8	< 1	1.45	0.520
488413	10	58	138	< 0.3	1.3	< 2	1.4	< 1	3.07	0.370
488414	1	< 3	< 1	< 0.3	< 0.3	< 2	0.5	< 1	0.13	0.240
488415	9	2630	184	5.7	0.7	< 2	5.6	< 1	0.47	0.320
488416	9	271	< 1	5.0	< 0.3	< 2	6.5	< 1	0.33	0.270
488417	1	12	< 1	< 0.3	< 0.3	< 2	0.7	< 1	0.14	0.400
488418	171	141000	90	401.0	1.1	8	487.0	5	0.35	2.210
488419	93	109000	< 1	180.0	0.5	6	127.0	< 1	0.43	1.530
488420	78	85400	85	76.9	0.5	9	76.1	< 1	0.47	1.130
488421	566	411000	< 1	1570.0	1.5	19	2730.0	< 1	0.20	6.340
488422	49	3100	< 1	< 0.3	< 0.3	< 2	14.9	< 1	5.20	1.150
488423	91	997	100	< 0.3	< 0.3	< 2	6.4	< 1	8.10	1.050
488424	7	78	< 1	< 0.3	< 0.3	< 2	1.4	< 1	2.76	3.220
488425	6	192	< 1	< 0.3	< 0.3	< 2	1.7	< 1	1.81	1.610
488426	9	21	70	< 0.3	< 0.3	< 2	0.5	< 1	2.76	0.370
488427	25	67	127	< 0.3	< 0.3	< 2	0.6	< 1	2.77	0.020
488428	30	62	< 1	< 0.3	< 0.3	< 2	0.7	< 1	31.70	> 20.0
488429	3	43	154	< 0.3	< 0.3	< 2	0.2	< 1	1.64	0.130
488430	4	94	150	< 0.3	0.4	< 2	3.2	< 1	1.84	0.070
488431	5	86	< 1	< 0.3	< 0.3	< 2	1.8	< 1	1.41	0.020
488432	78000	23600	4140	55.0	26.5	< 2	50.5	< 1	7.21	8.710
488433	911	15200	132000	< 0.3	737.0	< 2	9.1	< 1	0.36	7.020
488434	10300	3190	400	< 0.3	1.5	< 2	5.5	< 1	1.35	0.830
488435	15900	895	1580	< 0.3	16.2	< 2	5.8	< 1	2.19	0.790
488436	39700	378	2960	88.0	27.5	< 2	288.0	< 1	1.12	0.770
488437	39700	2120	8980	83.0	44.7	< 2	271.0	< 1	0.66	0.420
488438	141	38700	88	14.0	< 0.3	< 2	39.1	< 1	0.78	0.870
488439	40	715	< 1	< 0.3	< 0.3	< 2	5.5	< 1	0.23	0.230
488440	12	208000	< 1	61.0	0.5	< 2	244.0	4	1.20	3.550
488441	3	1340	< 1	< 0.3	< 0.3	< 2	0.8	< 1	0.11	0.800
488442	7	2110	< 1	6.0	< 0.3	< 2	11.7	< 1	0.65	0.170
488443	22	50	90	< 0.3	< 0.3	< 2	0.6	< 1	2.69	0.840
488444	4	54	90	< 0.3	< 0.3	< 2	0.8	< 1	2.71	0.930
488445	17	223	188	< 0.3	0.4	< 2	2.2	< 1	9.07	10.200
488446	7	39	75	< 0.3	< 0.3	< 2	0.6	< 1	2.44	1.240
488447	64	54	100	< 0.3	< 0.3	< 2	0.7	< 1	6.85	3.900
488448	10	4240	3400	20.0	20.0	46	0.7	< 1	3.11	1.520

Table 2. Analytical results

GGU no.	Cu ppm	Pb ppm	Zn ppm	Ag ppm	Cd ppm	Bi ppm	Sb ppm	Hg ppm	Fe pct	S pct
488449	6	< 3	< 1	< 0.3	< 0.3	< 2	< 0.1	< 1	1.18	0.120
488450	6	6	91	< 0.3	< 0.3	< 2	< 0.1	< 1	1.51	0.490
488451	4	45	< 1	< 0.3	< 0.3	< 2	0.3	< 1	0.39	0.120
488452	11	16	< 1	< 0.3	< 0.3	< 2	0.3	< 1	0.81	0.010
488453	75600	143000	175	327.0	2.8	< 2	0.3	3	0.53	5.340
488601	575	73	416000	< 0.3	1660.0	< 2	39.0	28	0.52	> 20.0
488602	316	712	27500	< 0.3	92.8	< 2	1.6	< 1	0.49	1.070
488603	225	411	195	< 0.3	< 0.3	< 2	0.6	< 1	7.08	0.630
488604	8	26	667	< 0.3	2.3	< 2	0.6	< 1	1.39	0.610
488605	12	< 3	188	< 0.3	0.5	< 2	< 0.1	< 1	0.88	0.190
488606	51	52	234	< 0.3	0.3	< 2	< 0.1	< 1	2.35	0.150
488607	4	76	< 1	< 0.3	< 0.3	< 2	2.3	< 1	0.57	0.110
488608	20	9	218	< 0.3	0.4	< 2	0.9	< 1	1.85	0.020
488609	6	< 3	160	< 0.3	< 0.3	< 2	< 0.1	< 1	1.93	0.050
488610	7	< 3	< 1	< 0.3	< 0.3	< 2	1.0	< 1	2.19	2.770
488611	6	< 3	< 1	< 0.3	< 0.3	< 2	0.5	< 1	1.63	< 0.01
488612	4150	72600	30700	35.0	137.0	< 2	102.0	13	0.88	3.330
488613	1530	393	56700	< 0.3	223.0	< 2	13.8	9	0.57	2.490
488614	177	335	290	< 0.3	1.1	8	0.8	< 1	6.12	0.120
488615	1150	49	234	< 0.3	2.1	< 2	3.7	< 1	0.36	0.090
488616	11	97	< 1	< 0.3	< 0.3	< 2	2.3	< 1	1.32	0.020
488617	7	24	104	< 0.3	< 0.3	< 2	0.4	< 1	0.78	0.010
488618	15	72	107	< 0.3	0.8	5	0.6	< 1	1.09	0.020
488619	17	< 3	< 1	< 0.3	< 0.3	< 2	0.5	< 1	0.71	0.700
488620	5	19	60	< 0.3	< 0.3	< 2	< 0.1	< 1	0.58	< 0.01
488621	401	66400	< 1	8.0	< 0.3	< 2	< 0.1	< 1	0.33	0.060
488622	14200	362	1050	110.0	10.0	< 2	176.0	< 1	1.22	1.320
488623	106	52	< 1	< 0.3	< 0.3	< 2	1.2	< 1	1.02	0.070
488624	25	125	< 1	< 0.3	< 0.3	< 2	0.5	< 1	0.39	0.040
488625	88	19	< 1	< 0.3	< 0.3	< 2	1.1	< 1	0.04	8.650
488626	31	39	97	< 0.3	< 0.3	< 2	0.6	< 1	2.83	0.100
488627	21	16	< 1	< 0.3	< 0.3	< 2	0.2	< 1	0.10	0.050
488628	28100	33600	< 1	97.0	0.5	5	0.2	< 1	0.27	0.710
Samples	81	81	81	81	81	81	81	81	81	81
Minimum	1	< 3	< 1	< 0.3	< 0.3	< 2	< 0.1	< 1	0.04	< 0.01
Maximum	78000	411000	416000	1570.0	1660.0	46	2730.0	28	31.70	> 20.0

Table 2. Analytical results

GGU no.	Ba ppm	Ca pct	Mg pct	Mn ppm	Al pct	Na pct	K pct	Rb ppm	Sr ppm	Br ppm
488401	< 50	0.05	0.03	74	0.22	0.02	0.18	< 15	5	< 0.5
488402	< 50	2.10	0.42	4190	1.56	3.57	4.67	175	37	< 0.5
488403	< 50	0.24	0.02	102	2.00	2.50	4.66	320	17	< 0.5
488404	< 50	0.33	0.07	559	2.50	0.44	3.67	339	16	< 0.5
488405	< 50	0.35	0.07	506	2.66	1.14	3.77	339	15	< 0.5
488406	530	0.62	0.64	2080	1.94	3.81	5.17	158	125	< 0.5
488407	< 50	0.02	< 0.01	40	1.83	3.73	4.79	183	3	< 0.5
488408	53100	10.90	0.05	65	0.14	0.02	0.04	< 15	2220	< 0.5
488409	340	33.50	0.14	141	0.03	< 0.01	0.03	< 15	791	< 0.5
488410	306000	0.78	0.24	436	0.11	< 0.01	0.05	< 15	1740	< 0.5
488411	99000	12.70	4.53	2410	0.41	0.03	0.30	< 15	3950	< 0.5
488412	78900	3.70	1.40	1130	0.99	0.02	0.80	40	4400	< 0.5
488413	105000	12.00	6.12	3800	0.20	0.03	0.13	< 15	3260	< 0.5
488414	364600	1.05	0.34	85	0.03	< 0.01	0.01	< 15	3260	< 0.5
488415	181000	1.08	0.13	251	0.24	0.02	0.11	< 15	3750	0.7
488416	285000	0.68	0.34	145	0.18	0.01	0.13	< 15	2360	< 0.5
488417	304000	8.85	0.06	961	0.05	< 0.01	0.02	< 15	4840	< 0.5
488418	71300	0.12	0.03	339	0.25	0.03	0.16	< 15	410	< 0.5
488419	56100	0.05	0.03	36	0.23	0.03	0.14	< 15	484	< 0.5
488420	55100	0.16	0.05	92	0.34	0.03	0.23	< 15	847	< 0.5
488421	20000	0.02	0.02	35	0.13	0.05	0.09	< 15	185	< 0.5
488422	830	4.74	2.24	1510	3.56	3.21	1.46	63	644	< 0.5
488423	970	8.61	5.83	1960	3.72	0.20	2.73	130	781	< 0.5
488424	310	0.04	0.02	95	0.88	2.91	4.13	107	14	< 0.5
488425	230	0.02	0.21	103	2.34	1.42	5.90	209	24	< 0.5
488426	730	0.15	0.46	884	1.99	2.82	4.54	153	61	< 0.5
488427	660	2.12	0.78	2430	1.98	0.93	4.55	159	54	< 0.5
488428	< 50	3.77	0.95	5270	0.61	< 0.01	0.01	< 15	67	< 0.5
488429	500	18.00	0.03	1440	1.13	0.05	4.31	147	145	< 0.5
488430	330	7.70	0.04	1530	0.85	0.24	2.93	96	63	< 0.5
488431	< 50	12.10	0.09	264	1.14	1.83	1.25	95	86	< 0.5
488432	< 50	0.07	0.01	22	0.11	0.03	0.06	< 15	41	< 0.5
488433	400	0.34	< 0.01	90	0.13	0.02	0.03	< 15	50	< 0.5
488434	35000	0.82	0.02	388	0.18	0.02	0.08	< 15	5810	< 0.5
488435	270	14.20	0.05	2710	0.08	0.02	0.04	< 15	92	< 0.5
488436	1140	5.75	0.07	1800	0.42	0.02	0.38	< 15	149	< 0.5
488437	26400	0.73	0.06	130	0.44	0.01	0.30	< 15	1150	< 0.5
488438	300000	6.00	2.52	1550	0.07	0.02	0.03	< 15	1800	< 0.5
488439	360000	1.56	0.49	330	0.02	0.01	< 0.01	< 15	1280	< 0.5
488440	140000	8.23	4.09	2740	0.08	0.02	0.05	< 15	606	< 0.5
488441	210000	9.93	0.06	919	0.03	0.02	< 0.01	< 15	5350	< 0.5
488442	250000	2.07	0.80	738	0.20	0.02	0.08	< 15	2190	< 0.5
488443	2100	2.69	0.42	803	1.78	3.70	3.90	168	1070	< 0.5
488444	1600	2.97	0.28	1120	1.16	3.57	3.76	126	864	< 0.5
488445	480	4.93	0.95	3290	1.58	2.45	1.58	78	391	< 0.5
488446	1600	1.65	0.19	1530	1.70	3.28	6.12	212	357	< 0.5
488447	620	0.27	0.13	539	1.49	4.18	0.76	< 15	172	< 0.5
488448	240	22.40	0.45	1710	1.33	0.02	1.14	53	361	< 0.5

Table 2. Analytical results

GGU no.	Ba ppm	Ca pct	Mg pct	Mn ppm	Al pct	Na pct	K pct	Rb ppm	Sr ppm	Br ppm
488449	230	0.47	0.04	475	2.07	1.34	5.45	363	24	< 0.5
488450	< 50	0.44	0.03	2930	1.28	0.47	2.54	446	16	< 0.5
488451	330	1.51	0.03	359	2.10	0.96	5.85	406	24	< 0.5
488452	310	0.37	< 0.01	410	1.16	2.57	4.31	793	8	< 0.5
488453	900	0.12	0.09	35	0.81	1.41	2.57	81	254	< 0.5
488601	< 50	0.01	< 0.01	29	0.03	0.02	0.07	44	3	< 0.5
488602	190	0.47	0.15	130	0.29	0.03	0.16	< 15	16	< 0.5
488603	1700	8.57	4.43	1430	3.70	1.13	2.14	106	1930	< 0.5
488604	760	0.07	0.28	95	2.35	2.14	6.15	128	45	< 0.5
488605	450	0.04	0.10	31	2.14	1.78	4.89	186	21	< 0.5
488606	470	0.20	0.11	1140	2.11	0.73	5.66	203	28	< 0.5
488607	500	0.02	0.21	95	1.77	0.21	6.36	245	19	< 0.5
488608	360	0.06	0.05	549	2.01	2.07	3.85	140	13	< 0.5
488609	400	0.04	0.04	83	1.97	0.59	6.20	174	17	< 0.5
488610	200	0.04	0.02	166	1.77	0.03	0.61	< 15	31	< 0.5
488611	420	0.25	0.17	946	1.97	3.60	2.15	< 15	90	< 0.5
488612	< 50	3.18	0.09	351	1.06	0.02	1.04	34	75	< 0.5
488613	< 50	0.04	0.02	60	0.34	0.02	0.22	< 15	10	< 0.5
488614	820	2.26	1.46	3080	3.93	0.09	2.04	96	377	< 0.5
488615	740	18.60	0.28	1040	1.07	0.27	1.20	< 15	210	< 0.5
488616	130	1.57	0.47	331	2.24	0.06	4.07	722	23	< 0.5
488617	100	6.20	0.52	664	2.53	0.05	3.71	555	258	< 0.5
488618	< 50	3.58	0.11	3540	0.85	0.03	1.50	284	47	< 0.5
488619	< 50	0.71	0.08	271	1.61	0.92	5.78	478	27	< 0.5
488620	620	0.96	0.28	258	1.68	0.92	5.20	389	99	< 0.5
488621	1200	0.20	0.16	67	1.77	2.01	4.26	101	617	0.5
488622	144000	5.45	0.14	449	0.71	0.02	0.55	< 15	4370	< 0.5
488623	780	21.30	4.48	585	0.92	1.08	0.26	< 15	1570	< 0.5
488624	250	21.40	0.29	918	0.95	0.51	0.96	< 15	689	0.6
488625	1000	9.58	0.03	39	0.04	0.03	0.04	< 15	1140	< 0.5
488626	610	11.60	3.19	1020	4.28	3.46	0.80	< 15	825	< 0.5
488627	< 50	33.50	0.23	1340	0.05	0.01	0.07	< 15	239	< 0.5
488628	7400	5.99	0.07	1170	1.27	1.66	2.16	61	755	< 0.5
Samples	81	81	81	81	81	81	81	81	81	81
Minimum	< 50	0.01	< 0.01	22	0.02	< 0.01	< 0.01	< 15	3	< 0.5
Maximum	364600	33.50	6.12	5270	4.28	4.18	6.36	793	5810	0.7

Table 2. Analytical results

GGU no.	Mo ppm	W ppm	Sn pct	Ta ppm	Be ppm	Hf ppm	Y ppm	Cs ppm	U ppm	Th ppm
488401	< 1	< 1	< 0.01	< 0.5	< 1	< 1	< 1	< 1	< 0.5	0.7
488402	2210	< 1	0.08	23.8	24	37	53	< 1	10.8	101.0
488403	208	9	< 0.01	34.5	14	14	29	3	4.7	32.0
488404	< 1	13	< 0.01	17.0	9	8	49	5	14.1	38.1
488405	< 1	8	< 0.01	20.5	9	7	51	3	15.4	52.4
488406	< 1	< 1	< 0.01	12.4	7	14	10	< 1	6.6	19.2
488407	< 1	< 1	< 0.01	17.6	7	17	11	< 1	10.6	22.4
488408	< 1	< 1	< 0.01	< 0.5	< 1	< 1	< 1	< 1	< 0.5	2.0
488409	< 1	< 1	< 0.01	< 0.5	< 1	< 1	< 1	< 1	< 0.5	< 0.2
488410	< 1	< 1	< 0.01	< 0.5	< 1	< 1	< 1	< 1	< 0.5	1.2
488411	13	8	< 0.01	< 0.5	< 1	< 1	3	< 1	2.7	< 0.2
488412	18	< 1	< 0.01	0.8	< 1	< 1	4	< 1	< 0.5	2.8
488413	5	< 1	< 0.01	< 0.5	< 1	< 1	3	< 1	< 0.5	0.7
488414	< 1	< 1	< 0.01	< 0.5	< 1	< 1	< 1	< 1	< 0.5	< 0.2
488415	7	< 1	< 0.01	< 0.5	< 1	< 1	1	< 1	< 0.5	< 0.2
488416	10	< 1	< 0.01	< 0.5	< 1	< 1	< 1	< 1	< 0.5	1.1
488417	< 1	< 1	< 0.01	< 0.5	< 1	< 1	3	< 1	< 0.5	< 0.2
488418	< 1	< 1	< 0.01	< 0.5	< 1	< 1	1	< 1	< 0.5	1.6
488419	5	< 1	< 0.01	< 0.5	< 1	< 1	< 1	< 1	< 0.5	0.6
488420	5	< 1	< 0.01	< 0.5	< 1	< 1	1	< 1	< 0.5	1.4
488421	< 1	< 1	< 0.01	< 0.5	< 1	< 1	< 1	< 1	< 0.5	< 0.2
488422	6	< 1	< 0.01	2.6	3	7	20	4	3.1	9.8
488423	< 1	< 1	< 0.01	3.7	3	6	13	8	< 0.5	4.5
488424	11	< 1	< 0.01	6.7	6	16	12	< 1	5.4	8.1
488425	40	< 1	< 0.01	7.8	5	17	29	< 1	5.1	17.3
488426	< 1	4	< 0.01	3.9	3	6	13	< 1	1.3	5.8
488427	3	< 1	< 0.01	3.8	5	9	20	2	2.5	10.1
488428	< 1	< 1	< 0.01	< 0.5	2	< 1	8	2	0.9	1.1
488429	3	< 1	< 0.01	8.1	2	21	48	< 1	4.4	8.0
488430	700	< 1	< 0.01	10.7	3	23	43	< 1	9.0	20.1
488431	119	4	< 0.01	< 0.5	2	4	14	3	< 0.5	5.6
488432	10	< 1	< 0.01	< 0.5	< 1	< 1	< 1	< 1	< 0.5	< 0.2
488433	10	< 1	< 0.01	< 0.5	< 1	< 1	< 1	< 1	< 0.5	< 0.2
488434	3	< 1	< 0.01	< 0.5	< 1	< 1	3	< 1	2.9	1.0
488435	2	< 1	< 0.01	< 0.5	< 1	< 1	15	< 1	1.2	0.9
488436	5	< 1	< 0.01	< 0.5	< 1	< 1	12	< 1	9.8	4.6
488437	7	< 1	< 0.01	< 0.5	< 1	< 1	2	< 1	< 0.5	< 0.2
488438	< 1	< 1	< 0.01	< 0.5	< 1	< 1	2	< 1	< 0.5	0.8
488439	< 1	< 1	< 0.01	< 0.5	< 1	< 1	< 1	< 1	< 0.5	< 0.2
488440	< 1	< 1	0.04	< 0.5	< 1	< 1	2	< 1	< 0.5	< 0.2
488441	< 1	< 1	< 0.01	< 0.5	< 1	< 1	3	< 1	< 0.5	< 0.2
488442	10	< 1	< 0.01	< 0.5	< 1	< 1	1	< 1	< 0.5	< 0.2
488443	5	< 1	< 0.01	7.0	5	9	12	2	6.3	19.1
488444	< 1	< 1	< 0.01	7.3	5	7	13	< 1	4.7	16.7
488445	7	14	< 0.01	8.0	5	9	13	2	3.4	12.3
488446	6	< 1	< 0.01	6.9	4	10	5	< 1	3.2	16.6
488447	6	6	0.04	6.2	4	6	3	< 1	3.9	13.4
488448	< 1	< 1	< 0.01	< 0.5	2	1	17	2	< 0.5	1.8

Table 2. Analytical results

GGU no.	Mo ppm	W ppm	Sn pct	Ta ppm	Be ppm	Hf ppm	Y ppm	Cs ppm	U ppm	Th ppm
488449	1210	7	< 0.01	19.9	6	6	41	1	14.0	49.3
488450	987	3630	< 0.01	19.8	57	< 1	33	5	10.9	27.4
488451	1370	21	< 0.01	9.5	3	5	43	< 1	8.0	23.3
488452	4	9	0.01	54.8	9	8	10	6	12.1	27.7
488453	4	< 1	< 0.01	1.1	< 1	< 1	2	< 1	< 0.5	3.8
488601	12	< 1	< 0.01	< 0.5	< 1	< 1	< 1	< 1	< 0.5	< 0.2
488602	4	2	< 0.01	< 0.5	< 1	< 1	2	< 1	< 0.5	0.4
488603	< 1	< 1	< 0.01	4.7	2	4	24	13	< 0.5	3.7
488604	13	8	< 0.01	3.9	3	7	6	2	3.2	5.4
488605	< 1	< 1	< 0.01	9.2	6	26	33	< 1	4.5	16.0
488606	9	< 1	< 0.01	9.6	9	30	48	< 1	7.2	18.3
488607	39	14	0.02	6.7	4	8	21	1	5.2	12.2
488608	< 1	< 1	< 0.01	5.8	5	19	31	< 1	4.1	21.1
488609	< 1	< 1	< 0.01	9.7	5	31	53	1	7.1	17.9
488610	10	< 1	< 0.01	5.3	3	12	22	< 1	5.6	9.9
488611	< 1	< 1	< 0.01	11.5	14	13	26	2	6.7	21.2
488612	< 1	< 1	< 0.01	< 0.5	< 1	3	4	< 1	< 0.5	3.7
488613	5	< 1	< 0.01	< 0.5	< 1	< 1	< 1	< 1	< 0.5	1.1
488614	< 1	6	0.02	4.3	10	4	23	7	< 0.5	4.2
488615	< 1	< 1	< 0.01	< 0.5	< 1	1	5	< 1	1.7	3.0
488616	4	21	< 0.01	< 0.5	12	4	4	5	1.4	10.8
488617	< 1	279	< 0.01	0.8	7	3	11	2	1.1	5.7
488618	19	4580	< 0.01	1.2	4	< 1	19	3	1.8	5.0
488619	9670	54	< 0.01	16.4	21	5	85	3	19.9	43.7
488620	122	37	< 0.01	< 0.5	3	3	10	3	1.3	6.2
488621	6	11	< 0.01	< 0.5	1	2	2	< 1	6.0	6.7
488622	20	< 1	< 0.01	< 0.5	< 1	< 1	7	< 1	< 0.5	6.8
488623	14	< 1	< 0.01	< 0.5	< 1	2	10	< 1	2.4	2.8
488624	10	< 1	< 0.01	< 0.5	< 1	6	6	< 1	1.5	2.3
488625	< 1	< 1	< 0.01	< 0.5	< 1	< 1	< 1	< 1	< 0.5	< 0.2
488626	< 1	< 1	< 0.01	< 0.5	1	2	20	< 1	2.1	6.0
488627	< 1	< 1	< 0.01	< 0.5	< 1	< 1	3	< 1	0.5	< 0.2
488628	< 1	< 1	< 0.01	< 0.5	< 1	3	12	< 1	32.1	2.8
Samples	81	81	81	81	81	81	81	81	81	81
Minimum	< 1	< 1	< 0.01	< 0.5	< 1	< 1	< 1	< 1	< 0.5	< 0.2
Maximum	9670	4580	0.08	54.8	57	37	85	13	32.1	101.0

Table 2. Analytical results

GGU no.	Au ppb	As ppm	Se ppm	Ni ppm	Co ppm	Cr ppm	Ir ppb	Ti pct	V ppm	P pct
488401	< 2	4.4	< 3	< 1	37	< 2	< 5	0.02	3	0.004
488402	5	< 0.5	< 3	< 1	< 1	24	< 5	0.44	4	0.064
488403	< 2	8.4	< 3	< 1	< 1	< 2	< 5	0.05	< 2	< 0.001
488404	< 2	3.0	< 3	< 1	< 1	21	< 5	0.05	< 2	< 0.001
488405	< 2	3.8	< 3	< 1	< 1	< 2	< 5	0.07	2	0.004
488406	< 2	2.3	< 3	< 1	5	66	< 5	0.76	52	0.083
488407	< 2	94.9	< 3	< 1	< 1	< 2	< 5	0.50	9	0.023
488408	< 2	0.6	30	< 1	< 1	14	< 5	< 0.01	< 2	0.004
488409	< 2	0.9	< 3	< 1	< 1	< 2	< 5	< 0.01	< 2	0.013
488410	< 2	1.8	< 3	< 1	5	24	< 5	0.02	7	0.003
488411	< 2	14.1	< 3	< 1	9	23	< 5	0.05	23	0.021
488412	45	18.3	< 3	< 1	29	34	< 5	0.14	39	0.027
488413	< 2	2.3	< 3	< 1	4	16	< 5	0.03	14	0.013
488414	< 2	9.7	< 3	< 1	2	< 2	< 5	< 0.01	< 2	< 0.001
488415	< 2	10.1	< 3	< 1	5	47	< 5	0.03	13	0.009
488416	< 2	41.5	< 3	< 1	6	< 2	< 5	0.03	17	0.004
488417	< 2	0.9	< 3	< 1	< 1	< 2	< 5	< 0.01	4	0.004
488418	< 2	450.0	< 3	200	33	28	< 5	0.03	8	0.004
488419	< 2	268.0	< 3	96	19	47	< 5	0.03	9	0.005
488420	< 2	347.0	5	120	23	60	< 5	0.05	16	0.009
488421	< 2	378.0	< 3	140	29	< 2	< 5	0.01	4	0.002
488422	< 2	4.1	< 3	< 1	18	37	< 5	1.06	198	0.160
488423	< 2	4.8	< 3	145	54	292	< 5	2.65	386	0.135
488424	< 2	37.2	< 3	< 1	< 1	58	< 5	0.25	18	0.005
488425	6	11.5	< 3	< 1	< 1	17	< 5	0.31	9	0.016
488426	< 2	< 0.5	< 3	< 1	3	21	< 5	0.51	36	0.061
488427	< 2	2.7	< 3	< 1	6	48	< 5	0.44	58	0.041
488428	< 2	0.9	26	< 1	3	25	< 5	0.07	29	0.267
488429	< 2	1.3	< 3	< 1	< 1	22	< 5	0.11	2	0.008
488430	< 2	2.7	3	< 1	1	51	< 5	0.12	< 2	0.005
488431	< 2	1.9	< 3	< 1	4	60	< 5	0.35	102	0.023
488432	82	4160.0	< 3	760	152	58	< 5	< 0.01	< 2	0.004
488433	28	16.1	< 3	< 1	23	13	< 5	< 0.01	< 2	< 0.001
488434	9	192.0	< 3	90	43	77	< 5	0.02	5	0.006
488435	13	425.0	< 3	80	57	< 2	< 5	< 0.01	< 2	0.005
488436	< 2	6930.0	< 3	90	84	49	< 5	0.07	11	0.010
488437	< 2	7480.0	< 3	130	79	65	< 5	0.06	13	0.043
488438	< 2	18.3	< 3	< 1	< 1	< 2	< 5	< 0.01	4	0.006
488439	< 2	8.3	< 3	< 1	< 1	< 2	< 5	< 0.01	< 2	< 0.001
488440	< 2	5.3	< 3	< 1	1	< 2	< 5	0.01	5	0.010
488441	< 2	< 0.5	< 3	< 1	< 1	< 2	< 5	< 0.01	< 2	0.005
488442	< 2	2.8	< 3	< 1	2	< 2	< 5	0.03	11	0.004
488443	< 2	4.5	< 3	< 1	5	< 2	< 5	0.72	63	0.077
488444	< 2	3.2	< 3	< 1	5	< 2	< 5	0.65	60	0.061
488445	< 2	143.0	< 3	< 1	36	< 2	< 5	0.74	79	0.094
488446	< 2	8.6	< 3	< 1	6	9	< 5	0.51	46	0.051
488447	< 2	25.4	< 3	< 1	12	< 2	< 5	0.60	48	0.065
488448	< 2	13.9	9	< 1	14	29	< 5	0.10	47	0.026

Table 2. Analytical results

GGU no.	Au ppb	As ppm	Se ppm	Ni ppm	Co ppm	Cr ppm	Ir ppb	Ti pct	V ppm	P pct
488449	< 2	< 0.5	5	< 1	< 1	< 2	< 5	0.09	< 2	< 0.001
488450	< 2	2.7	< 3	< 1	< 1	< 2	< 5	0.04	< 2	< 0.001
488451	< 2	1.5	< 3	< 1	< 1	< 2	< 5	0.05	< 2	0.002
488452	< 2	< 0.5	< 3	< 1	< 1	6	< 5	0.02	3	< 0.001
488453	< 2	< 0.5	< 3	< 1	2	8	< 5	0.11	12	0.018
488601	< 2	< 0.5	< 3	< 1	56	< 2	< 5	< 0.01	< 2	0.002
488602	< 2	< 0.5	< 3	< 1	5	12	< 5	0.04	7	0.005
488603	< 2	< 0.5	< 3	< 1	35	94	< 5	1.59	258	0.163
488604	< 2	5.0	< 3	< 1	< 1	< 2	< 5	0.48	11	0.030
488605	< 2	< 0.5	< 3	< 1	< 1	< 2	< 5	0.30	15	0.004
488606	< 2	< 0.5	< 3	< 1	3	7	< 5	0.31	22	0.022
488607	6	36.6	< 3	< 1	< 1	< 2	< 5	0.14	7	0.005
488608	< 2	2.1	< 3	< 1	< 1	< 2	< 5	0.15	< 2	0.002
488609	< 2	1.4	3	< 1	1	< 2	< 5	0.26	10	0.015
488610	< 2	18.7	< 3	< 1	< 1	< 2	< 5	0.32	6	0.005
488611	< 2	2.6	< 3	< 1	3	< 2	< 5	0.23	14	0.034
488612	30	79.6	7	< 1	13	23	< 5	0.12	20	0.020
488613	< 2	38.7	5	< 1	7	16	< 5	0.03	3	0.002
488614	6	2.2	< 3	< 1	42	104	< 5	2.43	380	0.256
488615	< 2	88.6	< 3	< 1	7	15	< 5	0.09	13	0.016
488616	< 2	2.3	< 3	< 1	< 1	12	< 5	0.12	15	0.007
488617	< 2	3.0	< 3	< 1	< 1	11	< 5	0.11	17	0.021
488618	4	4.1	< 3	< 1	< 1	11	< 5	0.12	8	0.012
488619	< 2	3.3	< 3	< 1	< 1	7	< 5	0.05	< 2	0.005
488620	< 2	0.9	< 3	< 1	< 1	14	< 5	0.15	15	0.044
488621	7	< 0.5	< 3	< 1	< 1	17	< 5	0.19	34	0.035
488622	< 2	8840.0	< 3	< 1	17	13	< 5	0.09	28	0.022
488623	< 2	60.7	< 3	< 1	4	17	< 5	0.09	31	0.014
488624	< 2	9.8	< 3	< 1	2	18	< 5	0.10	15	0.051
488625	< 2	58.9	< 3	< 1	< 1	< 2	< 5	< 0.01	< 2	0.003
488626	5	5.9	< 3	< 1	9	61	< 5	0.41	120	0.067
488627	< 2	3.3	< 3	< 1	< 1	< 2	< 5	< 0.01	3	0.013
488628	< 2	2.0	< 3	< 1	< 1	< 2	< 5	0.07	20	0.017
Samples	81	81	81	81	81	81	81	81	81	81
Minimum	< 2	< 0.5	< 0.3	< 1	< 1	< 2	< 5	< 0.01	< 2	< 0.001
Maximum	82	8840.0	30	760	152	292	< 5	2.65	386	0.267

Table 2. Analytical results

GGU no.	La ppm	Ce ppm	Nd ppm	Sm ppm	Eu ppm	Tb ppm	Yb ppm	Lu ppm	Sc ppm	Mass g
488401	1.4	< 3	< 5	0.1	< 0.2	< 0.5	< 0.2	< 0.05	0.2	32.1
488402	162.0	246	65	14.9	1.3	< 0.5	15.7	2.41	4.9	32.4
488403	37.4	61	8	3.1	< 0.2	< 0.5	6.6	0.94	0.7	27.8
488404	84.1	143	34	8.3	< 0.2	1.4	7.7	1.15	0.8	25.9
488405	48.6	87	23	6.8	< 0.2	< 0.5	7.5	1.10	1.3	25.8
488406	135.0	214	74	12.3	1.8	< 0.5	4.7	0.76	5.5	27.2
488407	174.0	300	97	16.1	< 0.2	< 0.5	6.0	1.04	2.5	31.9
488408	2.3	4	< 5	0.2	< 0.2	< 0.5	< 0.2	< 0.05	0.2	31.5
488409	0.5	< 3	< 5	< 0.1	< 0.2	< 0.5	< 0.2	< 0.05	0.2	26.9
488410	2.6	< 3	< 5	0.2	< 0.2	< 0.5	< 0.2	0.15	1.1	33.5
488411	6.4	6	< 5	0.5	< 0.2	< 0.5	0.4	0.07	1.5	27.5
488412	10.3	14	< 5	0.9	< 0.2	< 0.5	0.7	0.14	1.9	26.4
488413	3.3	6	< 5	0.5	< 0.2	< 0.5	< 0.2	< 0.05	1.3	28.5
488414	1.6	< 3	< 5	< 0.1	< 0.2	< 0.5	< 0.2	< 0.05	0.2	40.8
488415	3.7	5	< 5	0.2	0.6	< 0.5	< 0.2	< 0.05	0.7	36.4
488416	4.8	< 3	< 5	0.2	< 0.2	< 0.5	< 0.2	< 0.05	0.8	50.9
488417	2.7	< 3	< 5	0.4	2.0	< 0.5	< 0.2	< 0.05	0.3	37.1
488418	3.4	< 3	< 5	0.2	< 0.2	< 0.5	< 0.2	< 0.05	0.4	43.9
488419	3.3	< 3	< 5	0.2	< 0.2	< 0.5	< 0.2	< 0.05	0.5	35.0
488420	5.2	5	< 5	0.3	0.5	< 0.5	< 0.2	< 0.05	0.7	39.2
488421	1.6	< 3	< 5	0.3	< 0.2	< 0.5	< 0.2	< 0.05	0.4	49.7
488422	58.4	101	41	8.2	2.3	< 0.5	2.5	0.43	11.6	28.9
488423	41.7	73	32	6.7	2.6	< 0.5	1.3	0.24	35.0	35.5
488424	39.1	73	25	6.8	0.6	< 0.5	7.3	1.08	2.2	29.4
488425	125.0	210	76	13.4	0.9	0.9	6.8	1.15	3.4	24.3
488426	86.6	136	60	11.3	3.9	< 0.5	3.2	0.45	4.9	21.5
488427	58.8	102	43	8.0	1.9	0.9	4.2	0.70	6.8	22.9
488428	7.2	12	< 5	0.8	0.9	< 0.5	0.7	0.11	2.1	44.5
488429	93.1	164	63	12.5	1.2	2.2	9.0	1.33	2.5	27.9
488430	60.7	112	38	10.9	1.6	2.1	9.1	1.35	5.3	25.7
488431	20.8	36	16	3.5	1.0	0.8	2.3	0.34	9.2	22.8
488432	0.9	< 3	< 5	0.1	< 0.2	< 0.5	< 0.2	< 0.05	0.2	29.7
488433	< 0.5	< 3	< 5	< 0.1	< 0.2	< 0.5	0.4	< 0.05	< 0.1	27.4
488434	2.3	4	< 5	0.4	0.3	< 0.5	0.3	< 0.05	0.6	29.2
488435	7.1	16	10	2.3	1.1	< 0.5	1.0	0.15	4.3	25.4
488436	8.3	< 3	< 5	1.9	< 0.2	< 0.5	< 0.2	< 0.05	6.6	23.8
488437	2.6	< 3	< 5	0.5	< 0.2	< 0.5	< 0.2	< 0.05	0.7	25.9
488438	2.0	6	< 5	0.1	< 0.2	< 0.5	< 0.2	< 0.05	0.3	36.7
488439	1.7	< 3	< 5	< 0.1	< 0.2	< 0.5	< 0.2	< 0.05	0.1	38.1
488440	2.4	< 3	< 5	0.1	0.6	< 0.5	0.5	< 0.05	0.6	35.4
488441	3.7	< 3	< 5	0.3	1.1	< 0.5	0.4	0.37	0.2	38.1
488442	3.0	7	< 5	0.1	< 0.2	< 0.5	0.3	< 0.05	0.6	32.8
488443	94.4	148	48	8.2	2.5	1.1	3.3	0.54	1.8	23.5
488444	89.1	136	44	7.3	2.2	0.8	2.8	0.42	1.7	28.8
488445	130.0	208	66	11.2	2.7	< 0.5	2.5	0.43	1.9	27.0
488446	58.6	85	30	5.3	1.8	< 0.5	3.2	0.52	2.0	23.5
488447	20.8	31	11	1.6	0.7	< 0.5	1.8	0.31	1.3	25.1
488448	11.5	24	12	2.3	0.8	< 0.5	1.5	0.24	2.9	23.6

Table 2. Analytical results

GGU no.	La ppm	Ce ppm	Nd ppm	Sm ppm	Eu ppm	Tb ppm	Yb ppm	Lu ppm	Sc ppm	Mass g
488449	11.4	28	13	4.2	0.2	0.9	7.0	1.05	1.1	29.4
488450	12.3	26	11	2.9	< 0.2	2.1	6.9	0.99	2.4	30.9
488451	18.4	41	25	6.1	< 0.2	1.2	4.9	0.80	0.8	25.1
488452	17.5	40	8	2.2	< 0.2	< 0.5	7.4	1.28	2.5	26.7
488453	7.0	12	< 5	0.7	0.3	< 0.5	0.5	0.11	0.8	23.7
488601	0.6	< 3	< 5	< 0.1	< 0.2	< 0.5	< 0.2	< 0.05	< 0.1	33.5
488602	3.0	4	< 5	0.5	0.3	< 0.5	< 0.2	< 0.05	0.4	30.5
488603	60.8	107	49	9.1	3.5	0.8	1.8	0.30	23.4	35.8
488604	18.6	22	< 5	1.2	0.5	< 0.5	2.8	0.51	4.9	20.9
488605	28.5	51	18	5.0	0.5	1.1	10.3	1.48	3.8	21.7
488606	83.5	138	56	12.4	1.3	2.1	10.7	1.71	4.4	26.3
488607	35.2	60	23	4.6	0.6	< 0.5	3.6	0.52	3.1	24.4
488608	117.0	188	76	15.6	0.4	1.9	7.9	1.15	0.9	21.6
488609	31.5	44	19	6.1	0.7	1.8	12.6	1.88	2.9	25.1
488610	21.8	35	11	2.4	< 0.2	0.7	4.9	0.77	1.0	29.0
488611	68.0	115	37	8.1	0.9	1.4	5.3	0.86	2.0	20.5
488612	12.5	19	< 5	1.1	0.4	< 0.5	0.4	< 0.05	1.9	29.3
488613	2.5	4	< 5	0.3	< 0.2	< 0.5	< 0.2	< 0.05	0.3	32.7
488614	54.0	97	37	8.7	2.9	< 0.5	2.4	0.40	22.4	27.4
488615	11.2	18	8	1.5	0.5	< 0.5	0.4	0.05	1.5	24.6
488616	36.4	64	23	4.4	0.9	< 0.5	0.7	< 0.05	4.0	26.7
488617	21.8	37	17	2.9	1.1	< 0.5	1.2	0.21	8.2	27.4
488618	20.7	26	< 5	2.4	0.7	0.7	2.3	0.31	1.9	32.0
488619	23.3	68	58	16.7	0.4	2.7	18.1	2.61	1.5	27.0
488620	42.0	69	27	4.1	0.6	< 0.5	1.2	0.21	1.9	29.6
488621	11.8	19	< 5	0.8	0.4	< 0.5	0.5	< 0.05	1.7	26.7
488622	14.2	17	< 5	1.1	< 0.2	< 0.5	< 0.2	0.17	2.4	21.0
488623	12.4	20	9	1.7	< 0.2	< 0.5	1.1	0.17	3.9	29.2
488624	8.1	13	5	1.2	0.4	< 0.5	0.8	0.17	2.1	25.7
488625	0.8	< 3	< 5	0.1	< 0.2	< 0.5	< 0.2	< 0.05	0.2	22.7
488626	29.2	47	14	3.6	0.8	< 0.5	1.7	0.29	10.2	26.2
488627	1.6	3	< 5	0.4	< 0.2	< 0.5	0.2	< 0.05	0.3	28.7
488628	20.3	30	10	3.2	1.1	0.6	1.4	0.21	1.2	27.5
Samples	81	81	81	81	81	81	81	81	81.0	81
Minimum	< 0.5	< 3	< 5	< 0.1	< 0.2	< 0.5	< 0.2	< 0.05	< 0.1	20.5
Maximum	174.0	300	97	16.7	3.9	2.7	18.1	2.61	35.0	50.9